

RESEARCH

Open Access



# Mathematical modeling and analysis of fractional-order brushless DC motor

Zain Ul Abadin Zafar<sup>1</sup>, Nigar Ali<sup>2</sup> and Cemil Tunç<sup>3\*</sup> 

\*Correspondence:

[cemtunc@yahoo.com](mailto:cemtunc@yahoo.com)

<sup>3</sup>Department of Mathematics,  
Faculty of Science, Van Yuzuncu Yil  
University, 65080, Van, Turkey  
Full list of author information is  
available at the end of the article

## Abstract

In this paper, we consider a fractional-order model of a brushless DC motor. To develop a mathematical model, we use the concept of the Liouville–Caputo noninteger derivative with the Mittag–Leffler kernel. We find that the fractional-order brushless DC motor system exhibits the character of chaos. For the proposed system, we show the largest exponent to be 0.711625. We calculate the equilibrium points of the model and discuss their local stability. We apply an iterative scheme by using the Laplace transform to find a special solution in this case. By taking into account the rule of trapezoidal product integration we develop two iterative methods to find an approximate solution of the system. We also study the existence and uniqueness of solutions. We take into account the numerical solutions for Caputo Liouville product integration and Atangana–Baleanu Caputo product integration. This scheme has an implicit structure. The numerical simulations indicate that the obtained approximate solutions are in excellent agreement with the expected theoretical results.

**MSC:** 34A08; 34D06; 34H10; 93C095; 93D05

**Keywords:** Brushless DC motor (BDCM); Chaotic attractor; Product integration; Atangana–Baleanu derivative; Liouville–Caputo derivative; Lyapunov exponent

## 1 Introduction

The newly emerging field has many applications to model the real-world phenomena such as electrode–electrolyte, diffusion wave, electromagnetic waves, dielectric polarization, and superdiffusion equations [1–3]. Similarly, a fractional-order system is used to model many complex chaotic behaviors such as noninteger-order gyroscopes [4]. Moreover, fractional-order models are used to model microelectromechanical structures [5]. Also, noninteger-order electronic circuits [6, 7], chaotic communications [8], and authenticated encryption schemes [9] have been modeled by using FDEs.

Moreover, BLDCM has many recompenses over brushed DC motor [10–13] and practiced generally in manufacturing industrial engineering and automation design, for example, ventilations and heating, radio-controlled cars, and motion control systems. Further, BLDCM reveals undesirable chaotic phenomena [11–16]. To find novel means to suppress and control chaos more competently, numerous researchers have paid more and more attention, for instance, to multiple controllers, multiple state variables, and the nonlinear

© The Author(s) 2021. This article is licensed under a Creative Commons Attribution 4.0 International License, which permits use, sharing, adaptation, distribution and reproduction in any medium or format, as long as you give appropriate credit to the original author(s) and the source, provide a link to the Creative Commons licence, and indicate if changes were made. The images or other third party material in this article are included in the article's Creative Commons licence, unless indicated otherwise in a credit line to the material. If material is not included in the article's Creative Commons licence and your intended use is not permitted by statutory regulation or exceeds the permitted use, you will need to obtain permission directly from the copyright holder. To view a copy of this licence, visit <http://creativecommons.org/licenses/by/4.0/>.

feedback controllers. However, these control strategies require heavy computational efforts and are difficult to use in practice [17, 18].

Fractional calculus has attracted the focus of many researchers in the modern century [19–34]. Solving the problems of fractional order is very complicated. Therefore many approximate methods have been taken into account in recent decades. Despite the range of approaches, innovative concepts are needed in this field. Another important feature of this is the existence of demarcations of the integrals and derivatives, among which the prevalent demarcations are Riemann–Liouville–Caputo [17], Hadamard [35], Hilfer [36], Atangana–Baleanu [37], and Gomez–Atangana [38]. The most valid definition is that of Atangana and Baleanu for fractional derivatives [24, 39–44]. These were demarcated as a convolution integral with a Mittag-Leffler kernel. The presence of this property in the definition makes it a resilient technique to retain the valuable facts of the phenomenon in memory over time. In the recent papers [45–55], various interesting qualitative results for a number of differential equations, fractional differential equations, impulsive differential equations, and so on are obtained, and some related examples are given. The novelty of this paper is that we are pioneers to use this latest technique on this model. The system is closely resembling to the Lorenz attractor. The simulations of the first example show the butterfly effect.

In this paper, we introduce BLDCM model of noninteger order, which displays the chaotic behavior too. The maximum Lyapunov exponent and chaotic attractors are found by numerical calculation. Next, we consider two numerical schemes for the stabilization of noninteger-order chaotic BLDCMs. We carry out numerical imitations to present authenticity, validity, and feasibility of the developed schemes.

## 2 Preliminaries

The noninteger derivative of function  $h(t)$  using the Riemann–Liouville operator is defined as

$${}^RL D_t^{\tau_1} [h(t)] = \frac{1}{\Gamma(n - \tau_1)} \frac{d^n}{dt^n} \int_0^t h(\xi) (t - \xi)^{n - \tau_1 - 1} d\xi, \quad n - 1 < \tau_1 \leq n \in N. \quad (1)$$

The Laplace transform of the Caputo derivative is given by

$${}^RL D_t^{\tau_1} [h(t)] = s^{\tau_1} H(s) - \sum_{j=0}^{n-1} s^j [{}_0 D_t^{\tau_1 - j - 1} h(t)], \quad n - 1 < \tau_1 \leq n \in N. \quad (2)$$

The noninteger derivative of a function  $h(t)$  using the Liouville–Caputo operator is defined as [20]

$${}^LC D_t^{\tau_1} [h(t)] = \frac{1}{\Gamma(n - \tau_1)} \int_0^t \frac{d[h(\xi)]}{dt} (t - \xi)^{n - \tau_1 - 1} d\xi, \quad n - 1 < \tau_1 \leq n \in N. \quad (3)$$

The Laplace transform of the Caputo derivative is given by

$${}^LC D_t^{\tau_1} [h(t)] = s^{\tau_1} H(s) - \sum_{j=0}^{n-1} s^{\tau_1 - j - 1} h^j(0), \quad n - 1 < \tau_1 \leq n \in N. \quad (4)$$

A new significant fractional Atangana–Baleanu Caputo derivative (FABC) was discussed in [38]:

$${}^{\text{ABC}}_0 D_t^{\tau_1} z(t) = \frac{Z(\tau_1)}{\Gamma(n - \tau_1)} \int_0^t \frac{d[h(\xi)]}{dt} E_{\tau_1} \left[ \frac{\tau_1(t - \xi)^{\tau_1}}{\tau_1 - n} \right] d\xi, \quad n - 1 < \tau_1 \leq n \in \mathbb{N}, \tag{5}$$

where  $Z(\tau_1)$  is a normalization function, and  $Z(0) = 1 = Z(1)$ . We can observe from the structure of this functional operator that the Mittag-Leffler fraction is applied. As we can see, in the system of this fractional operator the fraction of Mittag-Leffler is used, as this would make the definition have both nonsingular and nonlocal kernel properties, and  $E_{\tau_1}$  denotes the one-parameter Mittag-Leffler function expressed in terms of power series:

$$u(z) = E_{\tau_1}(z) = \sum_{j=0}^{\infty} \frac{z^j}{\Gamma(\tau_1 j + 1)}, \quad \tau_1 > 0. \tag{6}$$

The Mittag-Leffler function in two parameters has the following form:

$$E_{\tau_1, \tau_2}(z) = \sum_{j=0}^{\infty} \frac{z^j}{\Gamma(\tau_1 j + \tau_2)}, \quad \tau_1 > 0, \tag{7}$$

where  $\tau_1$  and  $\tau_2$  are arbitrary complex numbers. When  $\tau_1 > 0$  and  $\tau_2 = 1$ ,  $E_{\tau_1}(z) = E_{\tau_1, 1}(z)$ .

### 3 Mathematical model

The mathematical exemplary of brushless DC motor (BLDCM) [13, 18] with no loading conditions is given by

$$\begin{cases} D_t u_d(t) = -\sigma u_d + u_q u_a, \\ D_t u_q(t) = -u_q + \beta u_a - u_d u_a, \\ D_t u_a(t) = \gamma u_q - \gamma u_a. \end{cases} \tag{8}$$

The discrete axis current is denoted by  $u_d$ , whereas that quadrant axis current by  $u_q$ , and the angular velocity of the motor is denoted by  $u_a$ . Note that  $D_t = \frac{d}{dt}$ . Here the parameters  $\sigma$ ,  $\beta$ , and  $\gamma$  are calculated by the brushless DC motor type, and these are positive in nature. It was demonstrated that the structure (8) is chaotic when the parameters are

$$\sigma = 0.875, \quad \beta = 55, \quad \text{and} \quad \gamma = 4. \tag{9}$$

For the numerical simulation of the chaotic framework (8), we have taken (9) and the initial conditions as  $u_d(0) = 10$ ,  $u_q(0) = 10$ , and  $u_a(0) = 10$ .

The FBLDCM system in Liouville–Caputo sense is

$$\begin{cases} {}^{\text{LC}}_0 D_t^{\tau} u_d(t) = -\sigma u_d + u_q u_a, \\ {}^{\text{LC}}_0 D_t^{\tau} u_q(t) = -u_q + \beta u_a - u_d u_a, \\ {}^{\text{LC}}_0 D_t^{\tau} u_a(t) = \gamma u_q - \gamma u_a, \end{cases} \tag{10}$$

and, in the ABC sense, it is

$$\begin{cases} {}_0^{ABC}D_t^\tau u_d(t) = -\sigma u_d + u_q u_a, \\ {}_0^{ABC}D_t^\tau u_q(t) = -u_q + \beta u_a - u_d u_a, \\ {}_0^{ABC}D_t^\tau u_a(t) = \gamma u_q - \gamma u_a, \end{cases} \quad (11)$$

where  $0 < \tau \leq 1$  is the noninteger order.

#### 4 Chaotic system properties

In this segment, we dissect the chaotic framework (10) and detail its essential properties similar to dissipativity, equilibria, Lyapunov exponents, and Kaplan–Yorke dimension.

##### 4.1 Dissipativity

In vector notation, we may communicate the framework (10) as follows:

$$\begin{cases} {}_0^{LC}D_t^\tau u_d(t) = f_1(u_d, u_q, u_a), \\ {}_0^{LC}D_t^\tau u_q(t) = f_2(u_d, u_q, u_a), \\ {}_0^{LC}D_t^\tau u_a(t) = f_3(u_d, u_q, u_a), \end{cases} \quad (12)$$

where

$$\begin{cases} f_1(u_d, u_q, u_a) = -\sigma u_d + u_q u_a, \\ f_2(u_d, u_q, u_a) = -u_q + \beta u_a - u_d u_a, \\ f_3(u_d, u_q, u_a) = \gamma u_q - \gamma u_a. \end{cases} \quad (13)$$

Let  $\Omega$  be any set in  $R^3$  with smooth boundary, and, moreover, let  $\Omega(t) = \Phi_t(\Omega)$ , where  $\Phi_t$  is the flow of  $f = (f_1, f_2, f_3)$ .

Besides, let  $V(t)$  denote the volume of  $\Omega(t)$ . Then by Liouville's theorem we have

$$D^\tau = \int_{\Omega(t)} (\nabla \cdot f) du_d du_q du_a. \quad (14)$$

It is easy to see the divergence of the chaotic structure (10) as

$$\nabla \cdot f = \frac{\partial f_1}{\partial u_d} + \frac{\partial f_2}{\partial u_q} + \frac{\partial f_3}{\partial u_a} = -\sigma - 1 - \gamma = -\delta < 0, \quad (15)$$

where

$$\sigma + 1 + \gamma = \delta > 0, \quad (16)$$

as  $\sigma$  and  $\gamma$  are positive parameters. So the structure is dissipative. Substituting (15) into (14), we obtain

$$D^\tau = -\delta V(t). \quad (17)$$

To get the solution of (17), we need the following lemma.

**Lemma 1** ([56]) *Let  $u(t)$  be a continuous function on  $[t_0, \infty]$ , Suppose that*

$$\frac{d^\chi}{dt^\chi} g(t) \leq \mu - \lambda g(t), \quad g(t_0) = g_{t_0},$$

where  $0 < \chi < 1$ ,  $(\lambda, \mu) \in \mathbb{R}^2$ ,  $\lambda \neq 0$ , and  $t_0 \geq 0$  is the initial time. Then its elucidation has the arrangement

$$g(t) \leq \left( g_{t_0} - \frac{\mu}{\lambda} \right) E_\chi[-\lambda(t - t_0)] + \frac{\mu}{\lambda},$$

where  $E_\chi[z]$  is the Mittag-Leffler function with parameter  $\chi$ .

According to this lemma, we can say that the structure (10) is chaotic. Therefore the structure limit sets are eventually restricted into a specific limit set of zero volume, and the asymptotic motion of the chaotic structure (10) settles down onto an eccentric attractor of the framework.

### 5 Equilibrium points

The steadiness points of the chaotic structure (10) are achieved by deciphering the following system of equations:

$$\begin{cases} -\sigma u_d + u_q u_a = 0, \\ -u_q + \beta u_a - u_d u_a = 0, \\ \gamma u_q - \gamma u_a = 0. \end{cases} \tag{18}$$

We obtain three equilibrium points of systems (10) and (11):

$$\begin{cases} E_0 = (0, 0, 0), \\ E_1 = (\beta - 1, \sqrt{\sigma(\beta - 1)}, \sqrt{\sigma(\beta - 1)}), \\ E_2 = (\beta - 1, -\sqrt{\sigma(\beta - 1)}, -\sqrt{\sigma(\beta - 1)}). \end{cases} \tag{19}$$

The Jacobian of systems (10) and (11) at  $u^*$  is given by

$$J(u^*) = \begin{pmatrix} -\sigma & u_a^* & u_q^* \\ -u_a^* & -1 & \beta - u_d^* \\ 0 & \gamma & -\gamma \end{pmatrix}. \tag{20}$$

The Jacobian matrix at  $E_0$  is obtained as follows:

$$J(E_0) = \begin{pmatrix} -\sigma & 0 & 0 \\ 0 & -1 & \beta \\ 0 & \gamma & -\gamma \end{pmatrix}, \tag{21}$$

$$(\lambda + \sigma)(\lambda^2 + p_1 \lambda + p_2) = 0,$$

where  $p_1 = 1 + \gamma$ ,  $p_2 = \gamma - \beta\gamma$ .

So the three eigenvalues are

$$\begin{cases} \lambda_1 = -\sigma, \\ \lambda_2 = -\frac{\gamma}{2} - \frac{1}{2} + \frac{1}{2}\sqrt{4\beta\gamma + (\gamma - 1)^2}, \\ \lambda_3 = -\frac{\gamma}{2} - \frac{1}{2} - \frac{1}{2}\sqrt{4\beta\gamma + (\gamma - 1)^2}. \end{cases}$$

By the Routh–Hurwitz criteria the first root is  $\lambda_1 = -\sigma$ , whereas the other two can be obtained from  $\lambda^2 + p_1\lambda + p_2 = 0$ . Since the equation is quadratic in nature, for stability, the Routh–Hurwitz norms show that all the coefficients of the quadratic structure should be nonnegative. If  $p_2 > 0$ , then the threshold parameter  $R_0$  is less than 1. So

$$\gamma - \beta\gamma > 0, \quad 1 > \beta \implies R_0 = \beta < 1.$$

Since all the parameters are nonnegative and all the terms in  $p_1$  are positive, we have  $p_1 > 0$ . Then the Routh–Hurwitz norms ensure that  $E_0$  is locally asymptotically stable if  $\beta < 1$ .

The Jacobian matrix at  $E_1$  is

$$J(E_1) = \begin{pmatrix} -\sigma & \sqrt{\sigma(\beta - 1)} & \sqrt{\sigma(\beta - 1)} \\ -\sqrt{\sigma(\beta - 1)} & -1 & \beta - \beta + 1 \\ 0 & \gamma & -\gamma \end{pmatrix}. \tag{22}$$

**Definition 1** ([57]) The discriminant of a polynomial  $R(\lambda) = \lambda^3 + c_1\lambda^2 + c_2\lambda + c_3$  is defined as

$$D(p) = 18c_1c_2c_3 + (c_1c_2)^2 - 4c_3(c_1)^2 - 4(c_2)^3 - 27(c_3)^2. \tag{23}$$

The auxiliary equation of structure (14) about  $E_1$  is

$$\lambda^3 + c_1\lambda^2 + c_2\lambda + c_3 = 0, \tag{24}$$

where

$$c_1 = \gamma + \sigma + 1, \quad c_2 = \sigma\gamma + \sigma\beta, \quad c_3 = 2\sigma\gamma(\beta - 1). \tag{25}$$

**Theorem 1** For  $R_0 > 1$  in structure (3), the equilibrium point  $E_1$  is asymptotically stable if

$$D(p) > 0, \quad c_1c_2 > c_3, \quad \gamma \in (0, 1], \tag{26}$$

or

$$D(p) < 0, \quad \gamma \in \left(0, \frac{2}{3}\right], \tag{27}$$

where  $D(p)$ ,  $c_1$ ,  $c_2$ , and  $c_3$  are defined in (23) and (25).

*Proof* For  $D(p) > 0$ ,  $c_1c_2 > c_3$ ; then  $c_1 > 0$  and  $c_3 > 0$ , via the Routh–Hurwitz norms. Then  $|\arg(\lambda)| > \frac{q\pi}{2}$ , and the under observed system will be locally asymptotically stable about

$E_1$ . It is clear from that  $c_1 > 0$ ,  $c_2 > 0$ , and  $c_1 c_2 > c_3$ . Then the states for stability of the noninteger order framework are satisfied [24], and so  $E_1$  is locally asymptotically stable.

The Jacobian matrix at  $E_2$  is

$$J(E_1) = \begin{pmatrix} -\sigma & -\sqrt{\sigma(\beta - 1)} & -\sqrt{\sigma(\beta - 1)} \\ \sqrt{\sigma(\beta - 1)} & -1 & \beta - \beta + 1 \\ 0 & \gamma & -\gamma \end{pmatrix}. \tag{28}$$

The characteristic equation of (28) is given by (24) and (25). So  $E_1$  and  $E_2$  are stable when  $R_0 > 1$ . □

### 6 Lyapunov exponents and Kaplan–Yorke dimension

For the selected values (9), the Lyapunov exponents of the framework (8) are obtained via Matlab as

$$L_1 = 0.711625, \quad L_2 = -0.000227, \quad L_3 = -6.586898. \tag{29}$$

Since the spectrum of Lyapunov exponents (29) has a positive term  $L_1$ , it follows that the 3D system (8) is chaotic. The maximal Lyapunov exponent (MLE) of the framework (8) is  $L_1 = 0.711625$ . We accomplish that our 3D structure (8) is a highly chaotic framework. It can be observed from equation (9) that the totality of the Lyapunov exponents is not positive. This shows that structure (8) is dissipative. Moreover, the Kaplan–Yorke dimension of (8) is deliberated as

$$D_{KY} = 2 + \frac{L_1 + L_2}{|L_3|} = 2.1080,$$

which is fractional. See Fig. 1.

### 7 Brushless DC motor model using Liouville–Caputo noninteger derivative

Here the approximated result of the problem is calculated using the iterative process. This approach uses the Laplace transform and its inverse.

The Liouville–Caputo noninteger-order brushless DC motor exemplary is defined in equation (10). The model initial conditions are

$$u_{d,0} = u_d(0), \quad u_{q,0} = u_q(0), \quad u_{a,0} = u_a(0). \tag{30}$$

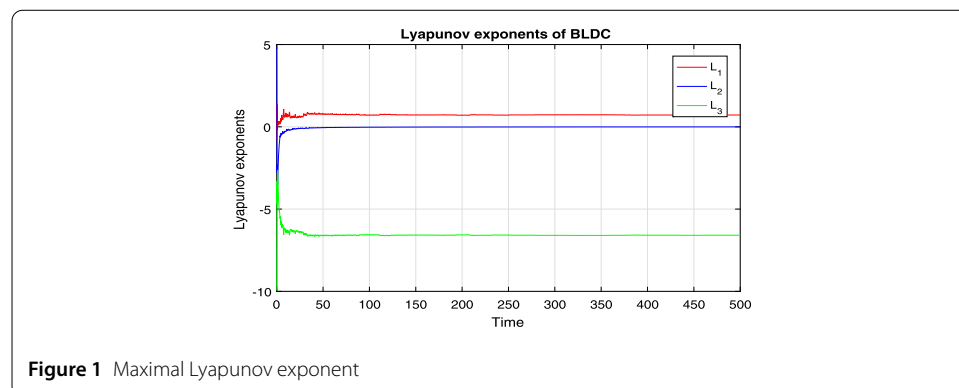


**Figure 1** Maximal Lyapunov exponent

After applying the Laplace transform to all sides of the Liouville–Caputo derivative specified by Eq. (3), we have [20]

$$L({}^{LC}D_t^\tau(U(t)))(p) = p^\tau U(p) - \sum_{k=0}^{m-1} p^{\tau-k-1} U^{(k)}(0). \tag{31}$$

The following iterative scheme is obtained by applying the Laplace transform to Eq. (31) and then applying the inverse Laplace transform to all sides of (10):

$$\begin{cases} u_{d,n}(t) - u_d(0) = L^{-1}(\frac{1}{p^\tau} L(-\sigma u_d(t) + u_q(t)u_a(t))(p))(t), \\ u_{q,n}(t) - u_q(0) = L^{-1}(\frac{1}{p^\tau} L(-u_q(t) + \beta u_a(t) - u_d(t)u_a(t))(p))(t), \\ u_{a,n}(t) - u_a(0) = L^{-1}(\frac{1}{p^\tau} L(\gamma u_q(t) - \gamma u_a(t))(p))(t) \end{cases} \tag{32}$$

with initial conditions (30).

The approximate solution is considered in the limit as  $n$  tends to infinity:

$$u_d = \lim_{n \rightarrow \infty} u_{d,n}, \quad u_q = \lim_{n \rightarrow \infty} u_{q,n} \quad \text{and} \quad u_a = \lim_{n \rightarrow \infty} u_{a,n}. \tag{33}$$

### 8 Stability study of equation (10)

Assume that there are three affirmative number  $A, B,$  and  $C$  such that for all  $0 \leq t \leq T \leq \infty, \|u_d(t)\| < A, \|u_q(t)\| < B,$  and  $\|u_a(t)\| < C.$  Now we define

$$Z = \left\{ \zeta : (a, b)(0, T) \rightarrow Z, \frac{1}{\Gamma(\tau)} \int (t - \eta)^{(\tau-1)} v(\eta) u(\eta) d\eta < \infty \right\}. \tag{34}$$

Now let us define the operator

$$\Theta(u_d, u_q, u_a) = \begin{cases} -\sigma u_d + u_q u_a, \\ -u_q + \beta u_a - u_d u_a, \\ \gamma u_q - \gamma u_a. \end{cases} \tag{35}$$

Then

$$\begin{aligned} & \Theta(u_d, u_q, u_a) - \Theta(u_{d,1}, u_{q,1}, u_{a,1}) \\ &= \begin{cases} -\sigma(u_d - u_{d,1}) + (u_q - u_{q,1})(u_a - u_{a,1}), \\ -(u_q - u_{q,1}) + \beta(u_a - u_{a,1}) - (u_d - u_{d,1})(u_a - u_{a,1}), \\ \gamma(u_q - u_{q,1}) - \gamma(u_a - u_{a,1}), \end{cases} \end{aligned}$$

where

$$u_d \neq u_{d,n}, \quad u_q \neq u_{q,n}, \quad \text{and} \quad u_a \neq u_{a,n}. \tag{36}$$

Now by the properties of the norm and absolute value we get

$$\begin{aligned}
 & \left( \Theta(u_d, u_q, u_a) - \Theta(u_{d,1}, u_{q,1}, u_{a,1}), (u_d - u_{d,1}, u_q - u_{q,1}, u_a - u_{a,1}) \right) \tag{37} \\
 & < \begin{cases} \left\{ -\sigma \left( \frac{\|u_d - u_{d,1}\|}{\|u_d - u_{d,1}\|^2} \right) + \left( \frac{\|u_q - u_{q,1}\|}{\|u_q - u_{q,1}\|^2} \right) \left( \frac{\|u_a - u_{a,1}\|}{\|u_a - u_{a,1}\|^2} \right) \right\} \|u_d - u_{d,1}\|^2, \\ \left\{ -\left( \frac{\|u_q - u_{q,1}\|}{\|u_q - u_{q,1}\|^2} \right) + \beta \left( \frac{\|u_a - u_{a,1}\|}{\|u_a - u_{a,1}\|^2} \right) - \left( \frac{\|u_d - u_{d,1}\|}{\|u_d - u_{d,1}\|^2} \right) \left( \frac{\|u_a - u_{a,1}\|}{\|u_a - u_{a,1}\|^2} \right) \right\} \|u_q - u_{q,1}\|^2, \\ \left\{ \gamma \left( \frac{\|u_q - u_{q,1}\|}{\|u_q - u_{q,1}\|^2} \right) - \gamma \left( \frac{\|u_a - u_{a,1}\|}{\|u_a - u_{a,1}\|^2} \right) \right\} \|u_a - u_{a,1}\|^2, \end{cases}
 \end{aligned}$$

where

$$\begin{aligned}
 & \left( \Theta(u_d, u_q, u_a) - \Theta(u_{d,1}, u_{q,1}, u_{a,1}), (u_d - u_{d,1}, u_q - u_{q,1}, u_a - u_{a,1}) \right) \tag{38} \\
 & < \begin{cases} A \|u_d - u_{d,1}\|^2, \\ B \|u_q - u_{q,1}\|^2, \\ C \|u_a - u_{a,1}\|^2 \end{cases}
 \end{aligned}$$

with

$$\begin{cases} A = \left\{ -\sigma \left( \frac{\|u_d - u_{d,1}\|}{\|u_d - u_{d,1}\|^2} \right) + \left( \frac{\|u_q - u_{q,1}\|}{\|u_q - u_{q,1}\|^2} \right) \left( \frac{\|u_a - u_{a,1}\|}{\|u_a - u_{a,1}\|^2} \right) \right\}, \\ B = \left\{ -\left( \frac{\|u_q - u_{q,1}\|}{\|u_q - u_{q,1}\|^2} \right) + \beta \left( \frac{\|u_a - u_{a,1}\|}{\|u_a - u_{a,1}\|^2} \right) - \left( \frac{\|u_d - u_{d,1}\|}{\|u_d - u_{d,1}\|^2} \right) \left( \frac{\|u_a - u_{a,1}\|}{\|u_a - u_{a,1}\|^2} \right) \right\}, \\ C = \left\{ \gamma \left( \frac{\|u_q - u_{q,1}\|}{\|u_q - u_{q,1}\|^2} \right) - \gamma \left( \frac{\|u_a - u_{a,1}\|}{\|u_a - u_{a,1}\|^2} \right) \right\}. \end{cases} \tag{39}$$

In view of a given nonzero vector  $(u_d, u_q, u_a)$ , by a similar routine as before we get

$$\begin{aligned}
 & \left( \Theta(u_d, u_q, u_a) - \Theta(u_{d,1}, u_{q,1}, u_{a,1}), (u_d - u_{d,1}, u_q - u_{q,1}, u_a - u_{a,1}) \right) \tag{40} \\
 & < \begin{cases} A \|u_d - u_{d,1}\| \|u_d\|, \\ B \|u_q - u_{q,1}\| \|u_q\|, \\ C \|u_a - u_{a,1}\| \|u_a\|. \end{cases}
 \end{aligned}$$

The iterative scheme stability can be observed by considering equations (38) and (40).

### 9 Uniqueness and existence

Let  $\Upsilon$  be bounded closed convex subset of a Banach space  $F$ . Let  $\mu : \Upsilon \rightarrow \Upsilon$  be a condensing map, where  $F$  has a fixed point in  $\Upsilon$ . We are interested in the IVP (initial value problem) on the cylinder  $\delta = (t, m) \in R \times F : t \in [0, T], x \in \Upsilon(0, \Omega)$  for some fixed  $T > 0$  and  $\Omega > 0$  and suppose that there exist  $\delta \in (0, \zeta)$ ,  $u_d, u_q, u_a, L_1 \in L_{1/\delta}([0, T], R^+)$ , and the functions  $u_{d,0}, u_{q,0}, u_{a,0} \in C(R, F) \cap L^1_{loc}(R, F)$  such that  $u_{d,0} + u_{d,1} = u_d, u_{q,0} + u_{q,1} = u_q$ , and  $u_{a,0} + u_{a,1} = u_a$  and the following conditions are satisfied:

1.  $u_{d,0}, u_{q,0}$ , and  $u_{a,0}$  are bounded and Lipschitz.
2.  $u_{d,1}, u_{q,1}$ , and  $u_{a,1}$  are compact and bounded.
3.  $|R(t, n) - R(t, z)| \leq L_1(t) \|n - z\|$  for all  $(t, n), (t, z) \in R$ .

Applying the Riemann–Liouville integral [58] to all sides of equation (10), we get the following system of integral equations:

$$\begin{cases} u_d(t) = u_d(0) + \frac{1}{\Gamma(\tau)} \int_0^t (t - \zeta)^{\tau-1} u_{d,0}(\zeta, u_d(\zeta)) d\zeta \\ \quad + \frac{1}{\Gamma(\tau)} \int_0^t (t - \zeta)^{\tau-1} u_{d,1}(\zeta, u_d(\zeta)) d\zeta, \\ u_q(t) = u_q(0) + \frac{1}{\Gamma(\tau)} \int_0^t (t - \zeta)^{\tau-1} u_{q,0}(\zeta, u_q(\zeta)) d\zeta \\ \quad + \frac{1}{\Gamma(\tau)} \int_0^t (t - \zeta)^{\tau-1} u_{q,1}(\zeta, u_q(\zeta)) d\zeta, \\ u_a(t) = u_a(0) + \frac{1}{\Gamma(\tau)} \int_0^t (t - \zeta)^{\tau-1} u_{a,0}(\zeta, u_a(\zeta)) d\zeta \\ \quad + \frac{1}{\Gamma(\tau)} \int_0^t (t - \zeta)^{\tau-1} u_{a,1}(\zeta, u_a(\zeta)) d\zeta. \end{cases} \tag{41}$$

**Theorem 2** *Based on Hypotheses 1 and 2, the IVP has at least one elucidation in the interval  $[0, T]$  according to the condition*

$$K = \frac{\nu \|L\|_{1/\nabla} T^M}{\Gamma(\tau)} < 1, \tag{42}$$

where  $M = \zeta - \nabla$  and  $\Upsilon = (\frac{1-\nabla}{\zeta-\nabla})^{1-\nabla}$ .

*Proof* Considering  $X$  such that  $\alpha(0) + 1/(\Gamma(\tau))\nu(\|Z_1\|_{1/\nabla} + \|Z_2\|_{1/\nabla})T^M \leq X$  and suppose that  $\Upsilon_\epsilon = n : \|n\| \leq X$ , the closed ball in the Banach space  $([0, T], F)$  with  $\sup \|\cdot\|$ .

Now, we consider  $n : \Upsilon_X \rightarrow$  a Banach space  $([0, T], F)$ ,  $n \rightarrow n(u_{d,0} + u_{d,1})$  along with

$$\begin{cases} u_{d,0}(t) = u_{d,0}(0) + \frac{1}{\Gamma(\tau)} \int_0^t (t - \zeta)^{\tau-1} u_{d,0}(\zeta, n(\zeta)) d\zeta, \\ u_{d,1}(t) = u_{d,1}(0) + \frac{1}{\Gamma(\tau)} \int_0^t (t - \zeta)^{\tau-1} u_{d,1}(\zeta, n(\zeta)) d\zeta, \\ u_{q,0}(t) = u_{q,0}(0) + \frac{1}{\Gamma(\tau)} \int_0^t (t - \zeta)^{\tau-1} u_{q,0}(\zeta, n(\zeta)) d\zeta, \\ u_{q,1}(t) = u_{q,1}(0) + \frac{1}{\Gamma(\tau)} \int_0^t (t - \zeta)^{\tau-1} u_{q,1}(\zeta, n(\zeta)) d\zeta, \\ u_{a,0}(t) = u_{a,0}(0) + \frac{1}{\Gamma(\tau)} \int_0^t (t - \zeta)^{\tau-1} u_{a,0}(\zeta, n(\zeta)) d\zeta, \\ u_{a,1}(t) = u_{a,1}(0) + \frac{1}{\Gamma(\tau)} \int_0^t (t - \zeta)^{\tau-1} u_{a,1}(\zeta, n(\zeta)) d\zeta. \end{cases} \tag{43}$$

Now we proved that  $u_d, u_q$ , and  $u_a$  are condensing, and we can demonstrate the presence of a fixed point of  $u_d, u_q$ , and  $u_a$ .

1. We need to prove that  $u_d(\Upsilon_\epsilon) \subset \Upsilon_\epsilon$ . From  $n \in \Upsilon_\epsilon$  we have

$$\begin{cases} \|u_d\| \leq |u_d(0)| + \frac{1}{\Gamma(\tau)} \int_0^t (t - \zeta)^{\tau-1} u_{d,0}(\zeta, n(\zeta)) d\zeta \\ \quad \leq |u_d(0)| + \frac{1}{\Gamma(\tau)} \int_0^t (t - \zeta)^{\tau-1} u_{d,0}(\zeta, n(\zeta)) d\zeta + \frac{1}{\Gamma(\tau)} \int_0^t (t - \zeta)^{\tau-1} u_{d,1}(\zeta, n(\zeta)) d\zeta \\ \quad \leq |u_d(0)| + \frac{1}{\Gamma(\tau)} (\int_0^t (t - \zeta)^{\frac{\tau-1}{1-\nabla}} d\zeta)^{1-\nabla} (\int_0^t G_1^{1/\nabla}(\zeta) d\zeta)^\nabla \\ \quad \quad + \frac{1}{\Gamma(\tau)} (\int_0^t (t - \zeta)^{\frac{\tau-1}{1-\nabla}} d\zeta)^{1-\nabla} (\int_0^t G_2^{1/\nabla}(\zeta) d\zeta)^\nabla, \end{cases}$$

$$\|u_d\| \leq |u_d(0)| + \frac{\nu_1(\|G_1\|_{1/\nabla} + \|G_2\|_{1/\nabla})}{\Gamma(\tau)} T^{M_1} \leq X_1. \tag{44}$$

Similarly, we have

$$\begin{cases} \|u_q\| \leq |u_q(0)| + \frac{\nu_2(\|G_{11}\|_{1/\nabla} + \|G_{22}\|_{1/\nabla})}{\Gamma(\tau)} T^{M_2} \leq X_2, \\ \|u_a\| \leq |u_a(0)| + \frac{\nu_3(\|G_{111}\|_{1/\nabla} + \|G_{222}\|_{1/\nabla})}{\Gamma(\tau)} T^{M_3} \leq X_3, \end{cases} \tag{45}$$

and therefore  $u_d(\Upsilon_\epsilon), u_q(\Upsilon_\epsilon), u_a(\Upsilon_\epsilon) \subset \Upsilon_\epsilon$ .

2. We need to prove that  $u_{d,0}$ ,  $u_{q,0}$ , and  $u_{a,0}$  are contractions. For  $n, z \in \Upsilon_\epsilon$ , we have

$$\begin{cases} \|u_{d,0}(t) - u_{d,1}(t)\| \leq \frac{1}{\Gamma(\tau)} \int_0^t (t - \zeta)^{\tau-1} K(\zeta) |n(\zeta) - z(\zeta)| d\zeta \\ \leq \frac{1}{\Gamma(\tau)} (\int_0^t (t - \zeta)^{\frac{\tau-1}{1-\nabla}})^{1-\nabla} (K^{1/\nabla}(\zeta) d\zeta)^\nabla \|n - z\| \leq \Phi_1 \|n - z\|, \\ \|u_{q,0}(t) - u_{q,1}(t)\| \leq \frac{1}{\Gamma(\tau)} \int_0^t (t - \zeta)^{\tau-1} K(\zeta) |n(\zeta) - z(\zeta)| d\zeta \\ \leq \frac{1}{\Gamma(\tau)} (\int_0^t (t - \zeta)^{\frac{\tau-1}{1-\nabla}})^{1-\nabla} (K^{1/\nabla}(\zeta) d\zeta)^\nabla \|n - z\| \leq \Phi_2 \|n - z\|, \\ \|u_{a,0}(t) - u_{a,1}(t)\| \leq \frac{1}{\Gamma(\tau)} \int_0^t (t - \zeta)^{\tau-1} K(\zeta) |n(\zeta) - z(\zeta)| d\zeta \\ \leq \frac{1}{\Gamma(\tau)} (\int_0^t (t - \zeta)^{\frac{\tau-1}{1-\nabla}})^{1-\nabla} (K^{1/\nabla}(\zeta) d\zeta)^\nabla \|n - z\| \leq \Phi_3 \|n - z\|, \end{cases} \tag{46}$$

where

$$\Phi_i = \frac{1}{\Gamma(\tau)} \nu_i \|L\|_{1/\nabla} T^{Mi} < 1 \quad \text{for } i = 1, 2, 3. \tag{47}$$

The overhead equation proves that  $u_{d,0}$ ,  $u_{q,0}$ , and  $u_{a,0}$  are contractions such that  $\|u_{d,0}(n) - u_{d,1}(n)\| \leq \Phi_1 \|n - z\|$ ,  $\|u_{q,0}(n) - u_{q,1}(n)\| \leq \Phi_2 \|n - z\|$ , and  $\|u_{a,0}(n) - u_{a,1}(n)\| \leq \Phi_3 \|n - z\|$ .

3. We need to prove that  $u_{d,1}$ ,  $u_{q,1}$ , and  $u_{a,1}$  are compact. For  $0 \leq l_1 \leq l_2 \leq T$ , we have

$$\begin{cases} \|u_{d,1}r(l_1) - u_{d,1}z(l_2)\| \\ \leq \frac{1}{\Gamma(\tau)} \left| \int_0^{l_2} (l_2 - \zeta)^{\tau-1} u_{d,1}(\zeta - n(\zeta)) d\zeta - \int_0^{l_1} (l_1 - \zeta)^{\tau-1} u_{d,1}(\zeta - n(\zeta)) d\zeta \right| \\ \leq \frac{1}{\Gamma(\tau)} \int_0^{l_1} ((l_1 - \zeta)^{\tau-1} - (l_2 - \zeta)^{\tau-1}) F_1(\zeta) d\zeta + \frac{1}{\Gamma(\tau)} \int_{l_1}^{l_2} (j_2 - \zeta)^{\tau-1} F_1(\zeta) d\zeta \\ \leq \frac{1}{\Gamma(\tau)} \left[ \int_0^{l_1} ((l_1 - \zeta)^{\tau-1} - (l_2 - \zeta)^{\tau-1})^{\frac{1}{1-\nabla}} d\zeta \right] (F_1^{1/\nabla}(\zeta) d\zeta)^\nabla + \\ \frac{1}{\Gamma(\tau)} \left( \int_{l_1}^{l_2} (j_2 - \zeta)^{\frac{\tau-1}{1-\nabla}} d\zeta \right)^{1-\nabla} (F_1^{1/\nabla}(\zeta) d\zeta)^\nabla \\ \leq \frac{\nu_1}{\Gamma(\tau)} \left[ l_1^{\frac{\tau-\nabla}{1-\nabla}} - l_2^{\frac{\tau-\nabla}{1-\nabla}} + (l_2 - l_1)^{\frac{\tau-\nabla}{1-\nabla}} \right]^{1-\nabla} \|F_1\|_{1/\nabla} + \frac{\nu_1}{\Gamma(\tau)} (l_2 - l_1)^{\tau-\nabla} \|F_1\|_{1/\nabla} \\ \leq \frac{\nu_1}{\Gamma(\tau)} \left[ (l_2 - l_1)^{\frac{\tau-\nabla}{1-\nabla}} \right]^{1-\nabla} \|F_1\|_{1/\nabla} + \frac{\nu_1}{\Gamma(\tau)} (l_2 - l_1)^{\tau-\nabla} \|F_1\|_{1/\nabla} \\ \leq \frac{2\nu_1 \|F_1\|_{1/\nabla}}{\Gamma(\tau)} (l_2 - l_1)^{\tau-\nabla}. \end{cases} \tag{48}$$

Following the same procedure, we get

$$\begin{cases} \|u_{q,1}r(l_1) - u_{q,1}z(l_2)\| \leq \frac{2\nu_2 \|F_{11}\|_{1/\nabla}}{\Gamma(\tau)} (l_2 - l_1)^{\tau-\nabla}, \\ \|u_{a,1}r(l_1) - u_{a,1}z(l_2)\| \leq \frac{2\nu_3 \|F_{11}\|_{1/\nabla}}{\Gamma(\tau)} (l_2 - l_1)^{\tau-\nabla}. \end{cases} \tag{49}$$

By the Arzelà–Ascoli principle [59] we infer that  $u(d, 1)(\Upsilon_\zeta)$ ,  $u(q, 1)(\Upsilon_\zeta)$ , and  $u(a, 1)(\Upsilon_\zeta)$  are relatively compact, which infers that  $u_{d,1}$ ,  $u_{q,1}$ , and  $u_{a,1}$  are compact.

Then  $u_{d,1}$ ,  $u_{q,1}$ , and  $u_{a,1}$  are compact, and  $u_{d,0}$ ,  $u_{q,0}$  and  $u_{a,0}$  are contractions and hence completely continuous [60], so the maps  $u_{d,0} + u_{d,1} = u_d$ ,  $u_{q,0} + u_{q,1} = u_q$ , and  $u_{a,0} + u_{a,1} = u_a$  are condensing on  $\Upsilon_\zeta$ , and thus we have the existence of fixed points of  $u_d$ ,  $u_q$ , and  $u_a$ .

4. We want to verify that the assumed IVP has the elucidation on the real interval  $[0, T]$ . For this, we are interested in Hypothesis 3, condition (47), and the map  $W$  specified by

$$\begin{cases} W[u_d(t)] = u_d(0) + \frac{1}{\Gamma(\tau)} \int_0^t (t - \zeta)^{\tau-1} u_d(\zeta, u_d(\zeta)), \\ W[u_q(t)] = u_q(0) + \frac{1}{\Gamma(\tau)} \int_0^t (t - \zeta)^{\tau-1} u_q(\zeta, u_q(\zeta)), \\ W[u_a(t)] = u_a(0) + \frac{1}{\Gamma(\tau)} \int_0^t (t - \zeta)^{\tau-1} u_a(\zeta, u_a(\zeta)). \end{cases} \tag{50}$$

For  $u_{d,0}, u_{d,1}, u_{q,0}, u_{q,1}, u_{a,0}, u_{a,1} \in \Upsilon_\zeta$ , we get

$$\begin{cases} |W[u_{d,0}(t)] - W[u_{d,1}(t)]| \leq \frac{1}{\Gamma(\tau)} \int_0^t (t - \zeta)^{\tau-1} |u_{d,0}(\zeta) - u_{d,1}(\zeta)| d\zeta, \\ \qquad \qquad \qquad \leq \frac{1}{\Gamma(\tau)} (\int_0^t (t - \zeta)^{\frac{\tau-1}{1-\nabla}} d\zeta)^{1-\nabla} (L_1^{1/\nabla} d\zeta)^\nabla, \\ |W[u_{d,0}(t)] - W[u_{d,1}(t)]| \leq \frac{T^{M_1} v_1 \|L_1\|_{1/\nabla}}{\Gamma(\tau)} |u_{d,0} - u_{d,1}|. \end{cases} \tag{51}$$

Following the same procedure, we have

$$\begin{cases} |W[u_{q,0}(t)] - W[u_{q,1}(t)]| \leq \frac{T^{M_2} v_2 \|L_2\|_{1/\nabla}}{\Gamma(\tau)} |u_{q,0} - u_{q,1}|, \\ |W[u_{a,0}(t)] - W[u_{a,1}(t)]| \leq \frac{T^{M_3} v_3 \|L_3\|_{1/\nabla}}{\Gamma(\tau)} |u_{a,0} - u_{a,1}|. \end{cases}$$

In the above cases, condition (47) is ensured. Thus the existence of the particular elucidation for the exemplary is verified. □

### 10 The proposed numerical technique for equation (10)

Here we take into account an important numerical arrangement, which is based on the special rule, called PI rule [61], for the solution of the Liouville–Caputo noninteger model (10).

Let us consider the Liouville–Caputo noninteger initial value problem

$${}^L C D_t^\tau U(t) = H(t, U(t)) \tag{52}$$

along with the initial condition  $U(t_0) = U_0$ , where  $H(t, U(t))$  is continuous.

Applying the integral operator (6) to all sides of equation (52) and utilizing the definition of the noninteger LC integral, we have the integral equation

$$U(t) - U(0) = \frac{1}{\Gamma(\tau)} \int_0^t H(\zeta, U(\zeta)) d\zeta, \tag{53}$$

which is a Volterra integral equation obtained by an integral operator applied to equation (52) utilizing the definition of the Caputo noninteger integral.

Taking  $t = t_n = nh$  in (53), where  $h$  is the step size, we get

$$U(t_n) - U(t_0) = \frac{1}{\Gamma(\tau)} \sum_0^{n-1} \int_{t_i}^{t_{i+1}} t_{i+1} (t_n - \zeta)^{\tau-1} H(\zeta, U(\zeta)) d\zeta. \tag{54}$$

Now we can estimate the function  $H(\zeta, U(\zeta))$  with the help of the first-order Lagrange interpolation:

$$H(\zeta, U(\zeta)) \approx H(t_{i+1}, U_{i+1}) + \frac{\zeta - t_{i+1}}{h} (H(t_{i+1}, U_{i+1}) - H(t_i, U_i)), \quad \zeta \in [t_i, t_{i+1}]. \tag{55}$$

The following Liouville–Caputo product-integration (LC-PI) formula is obtained by substituting (55) into (54) along with certain algebraic manipulations [62]:

$$U_n = U_0 + h^\tau \left( \Pi_n H(t_0, U_0) + \sum_{i=1}^n \Xi_{n-i} H(t_i, U_i) \right), \quad n \geq 1, \tag{56}$$

where

$$\begin{cases} \Pi_n = \frac{(n-1)^\tau - n^\tau (n-\tau-1)}{\Gamma(\tau+2)}, \\ \Xi_j = \begin{cases} \frac{1}{\Gamma(\tau+2)}, & j = 0, \\ \frac{(j-1)^{\tau+1} - 2j^{\tau+1} + (j+1)^{\tau+1}}{\Gamma(\tau+2)}, & j = 1, 2, \dots, n-1. \end{cases} \end{cases} \quad (57)$$

We use the well-known Newton–Raphson iterative method to evaluate  $U_n$  in equation (56). During the process, discrete convolutions are tested by considering the algorithm of the fast Fourier transform. One of the returns of this technique is the low computing cost, which is directly proportional to  $O(N \log^2 N)$  subject to  $O(N^2)$  as in some other prevalent discretization. The core concept was suggested in [63] and included in some recent papers [64–66].

### 11 Numerical implementations for LC-PI method on equation (10)

This section is devoted to numerical imitations for the time-fractional brushless DC motor (10) in the Liouville–Caputo sense. Let us consider the numerical arrangements (56) and (57) to system (10):

$$\begin{cases} u_{d,n} = u_{d,0} + h^\tau (\Pi_n (-\sigma u_{d,0} + u_{q,0} u_{a,0}) + \sum_{i=1}^n \Xi_{n-i} (-\sigma u_{d,i} + u_{q,i} u_{a,i})), \\ u_{q,n} = u_{q,0} + h^\tau (\Pi_n (-u_{q,0} + \beta u_{a,0} - u_{d,0} u_{a,0}) \\ \quad + \sum_{i=1}^n \Xi_{n-i} (-u_{q,i} + \beta u_{a,i} - u_{d,i} u_{a,i})), \\ u_{a,n} = u_{a,0} + h^\tau (\Pi_n (\gamma u_{q,0} - \gamma u_{a,0}) + \sum_{i=1}^n \Xi_{n-i} (\gamma u_{q,i} - \gamma u_{a,i})). \end{cases} \quad (58)$$

*Example 1* Taking the iterative arrangement (58), we consider the following values of the parameters [13, 18]:  $\sigma = 0.875$ ,  $\beta = 55$ , and  $\gamma = 4$  with initial conditions  $u_d(0) = 10$ ,  $u_q(0) = 10$ , and  $u_a(0) = 10$ . See Fig. 2.

*Example 2* Taking the iterative arrangement (58), we consider the following values of the parameters:  $\sigma = 0.875$ ,  $\beta = 25$ , and  $\gamma = 42$  with initial conditions  $u_d(0) = 20$ ,  $u_q(0) = 20$ , and  $u_a(0) = 20$ . See Fig. 3.

*Example 3* Taking the iterative arrangement (58), we consider the following values of the parameters:  $\sigma = 1.25$ ,  $\beta = 25$ , and  $\gamma = 42$  with initial conditions  $u_d(0) = 12$ ,  $u_q(0) = 4$ , and  $u_a(0) = 3$ . See Fig. 4.

*Example 4* Taking the iterative arrangement (58), we consider the following values of the parameters:  $\sigma = 0.875$ ,  $\beta = 0.786$ , and  $\gamma = 4$  with the initial conditions  $u_d(0) = 10$ ,  $u_q(0) = 10$ , and  $u_a(0) = 10$ . See Fig. 5.

### 12 Brushless DC motor model via AB–Caputo fractional derivative

The AB–Caputo fractional order brushless DC motor model is defined by equation (11). We will use it with the initial conditions given in (30).

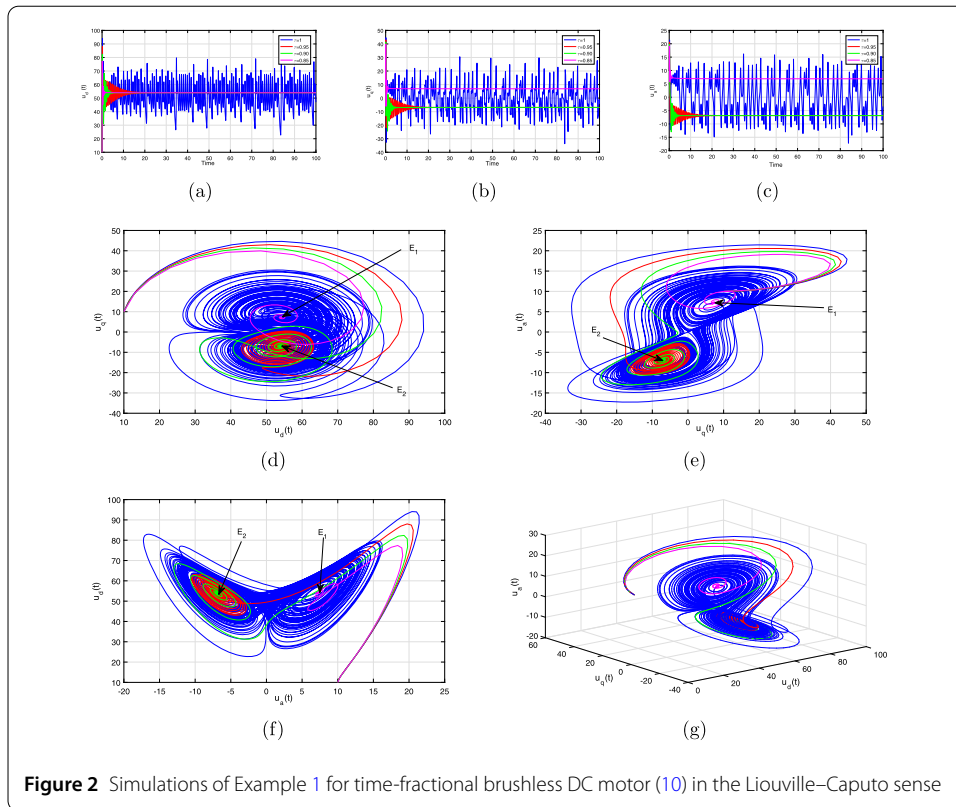


**Figure 2** Simulations of Example 1 for time-fractional brushless DC motor (10) in the Liouville–Caputo sense

### 12.1 Existence and uniqueness of elucidation of model (11) for the ABC-PI method

Using the noninteger integral operator of Atangana-Baleanu in equation (3), we have

$$\begin{cases} u_d(t) - u_d(0) = \frac{1-\tau}{Z(\tau)}(-\sigma u_d(t) + u_q(t)u_a(t)) \\ \quad + \frac{\tau}{Z(\tau)\Gamma(\tau)} \int_0^t (t-\zeta)^{\tau-1}(-\sigma u_d(\zeta) + u_q(\zeta)u_a(\zeta)) d\zeta, \\ u_q(t) - u_q(0) = \frac{1-\tau}{Z(\tau)}(-u_q(t) - u_d(t)u_a(t) + \beta u_a(t)) \\ \quad + \frac{\tau}{Z(\tau)\Gamma(\tau)} \int_0^t (t-\zeta)^{\tau-1}(-\sigma u_d(-u_q(\zeta) - u_d(\zeta)u_a(\zeta) + \beta u_a(\zeta)) d\zeta, \\ u_a(t) - u_a(0) = \frac{1-\tau}{Z(\tau)}(-\gamma u_a(t) + \gamma u_q(t)) \\ \quad + \frac{\tau}{Z(\tau)\Gamma(\tau)} \int_0^t (t-\zeta)^{\tau-1}(-\gamma u_a(\zeta) + \gamma u_q(\zeta)) d\zeta. \end{cases} \quad (59)$$

Let the kernels of system (59) be defined as

$$\begin{cases} K_1 = -\sigma u_d(t) + u_q(t)u_a(t), \\ K_2 = -u_q(t) - u_d(t)u_a(t) + \beta u_a(t), \\ K_3 = -\gamma u_a(t) + \gamma u_q(t). \end{cases} \quad (60)$$

First of all, we show that the kernels  $K_1, K_2,$  and  $K_3$  satisfy the Lipschitz condition.

**Theorem 3** *The kernels given in equation (60) satisfy the Lipschitz condition and contraction for  $0 \leq \eta_i < 1, i = 1, 2, 3.$*

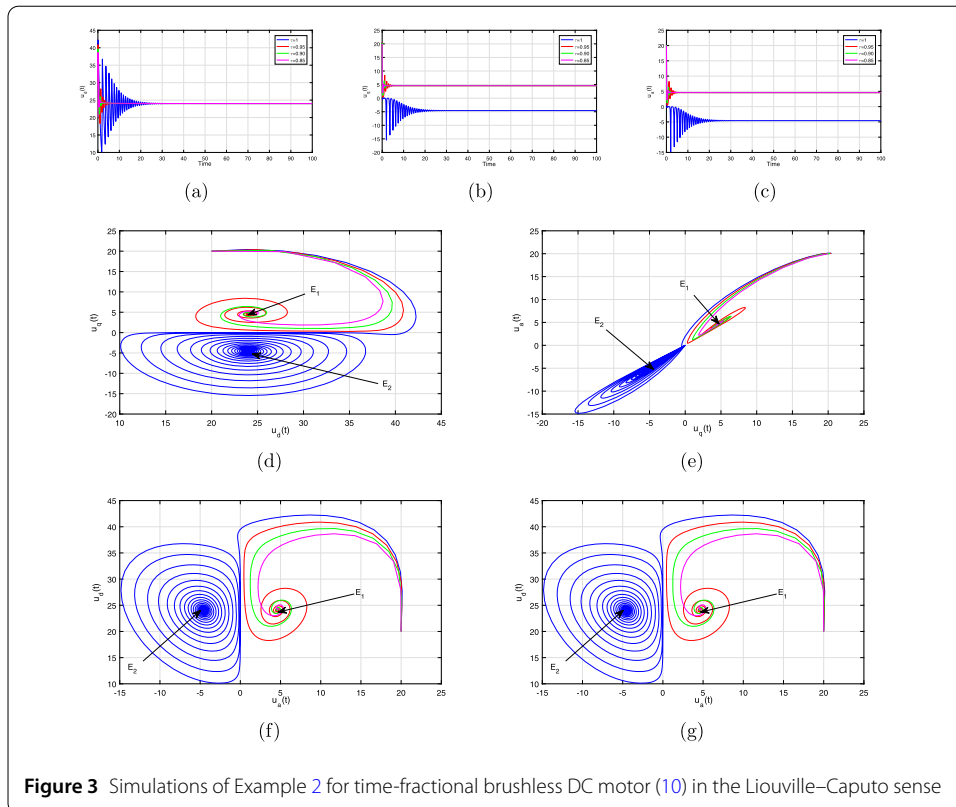


**Figure 3** Simulations of Example 2 for time-fractional brushless DC motor (10) in the Liouville–Caputo sense

*Proof* Consider the first equation from (60) and let  $u_d$  and  $u_{d,1}$  be two functions. Then

$$\begin{aligned} \|K_1(t, u_d) - K_1(t, u_{d,1})\| &= \|(u_q u_a - \sigma u_d) - (u_q u_a - \sigma u_{d,1})\| \\ &= \|\sigma u_{d,1} - \sigma u_d\| \\ &\leq \sigma \|u_{d,1} - u_d\| = \eta_1 \|u_{d,1} - u_d\|, \end{aligned}$$

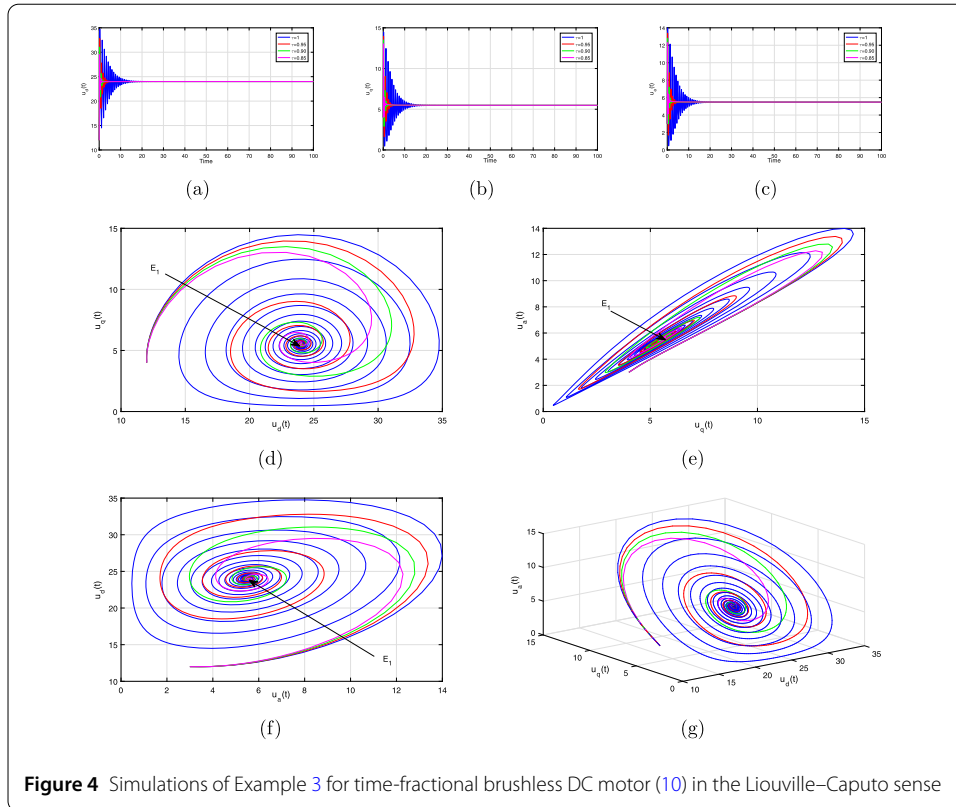
where  $\eta_1 = \sigma$ , that is,

$$\|K_1(t, u_d) - K_1(t, u_{d,1})\| \leq \eta_1 \|u_{d,1} - u_d\|, \tag{61}$$

which shows that the Lipschitz condition holds for  $K_1$ . Besides, if  $0 \leq \eta_1 < 1$ , then it also a contraction for  $K_1$ . Similarly, we obtain

$$\begin{aligned} \|K_2(t, u_q) - K_2(t, u_{q,1})\| &\leq \eta_2 \|u_{q,1} - u_q\|, \\ \|K_3(t, u_a) - K_3(t, u_{a,1})\| &\leq \eta_3 \|u_{a,1} - u_a\|. \end{aligned} \tag{62}$$

Now let  $l = K(m) \times m$ , and let  $K(m)$  be a Banach space of real-valued functions  $R \rightarrow R$  on  $m$  with the norm  $\|u_d, u_q, u_a\| = \|u_d\| + \|u_q\| + \|u_a\|$ , where  $\|u_d\| = \sup |u_d(t)| : t \in m$ ,  $\|u_q\| = \sup |u_q(t)| : t \in m$ , and  $\|u_a\| = \sup |u_a(t)| : t \in m$ . Equation (11) can be written in



the Volterra-type integral form as follows:

$$\begin{cases} u_d(t) - u_d(0) = \frac{1-\tau}{Z(\tau)}(-\sigma u_d(t) + u_q(t)u_a(t)) \\ \quad + \frac{\tau}{Z(\tau)\Gamma(\tau)} \int_0^t (t-\zeta)^{\tau-1}(-\sigma u_d(\zeta) + u_q(\zeta)u_a(\zeta)) d\zeta, \\ u_q(t) - u_q(0) = \frac{1-\tau}{Z(\tau)}(-u_q(t) - u_d(t)u_a(t) + \beta u_a(t)) \\ \quad + \frac{\tau}{Z(\tau)\Gamma(\tau)} \int_0^t (t-\zeta)^{\tau-1}(-\sigma u_d(-u_q(\zeta) - u_d(\zeta)u_a(\zeta) + \beta u_a(\zeta)) d\zeta, \\ u_a(t) - u_a(0) = \frac{1-\tau}{Z(\tau)}(-\gamma u_a(t) + \gamma u_q(t)) \\ \quad + \frac{\tau}{Z(\tau)\Gamma(\tau)} \int_0^t (t-\zeta)^{\tau-1}(-\gamma u_a(\zeta) + \gamma u_q(\zeta)) d\zeta. \end{cases} \quad (63)$$

Equation (63) can be written as

$$\begin{cases} u_d(t) - u_d(0) = \frac{1-\tau}{Z(\tau)}K_1(t, u_d) + \frac{\tau}{Z(\tau)\Gamma(\tau)} \int_0^t (t-\zeta)^{\tau-1}K_1(\zeta, u_d) d\zeta, \\ u_q(t) - u_q(0) = \frac{1-\tau}{Z(\tau)}K_2(t, u_q) + \frac{\tau}{Z(\tau)\Gamma(\tau)} \int_0^t (t-\zeta)^{\tau-1}K_2(\zeta, u_q) d\zeta, \\ u_a(t) - u_a(0) = \frac{1-\tau}{Z(\tau)}K_3(t, u_a) + \frac{\tau}{Z(\tau)\Gamma(\tau)} \int_0^t (t-\zeta)^{\tau-1}K_3(\zeta, u_a) d\zeta. \end{cases} \quad (64)$$

The recursive formula of equation (64) takes the following form:

$$\begin{cases} u_{d,n}(t) - u_d(0) = \frac{1-\tau}{Z(\tau)}K_1(t, u_{d,n-1}) + \frac{\tau}{Z(\tau)\Gamma(\tau)} \int_0^t (t-\zeta)^{\tau-1}K_1(\zeta, u_{d,n-1}) d\zeta, \\ u_{q,n}(t) - u_q(0) = \frac{1-\tau}{Z(\tau)}K_2(t, u_{q,n-1}) + \frac{\tau}{Z(\tau)\Gamma(\tau)} \int_0^t (t-\zeta)^{\tau-1}K_2(\zeta, u_{q,n-1}) d\zeta, \\ u_{a,n}(t) - u_a(0) = \frac{1-\tau}{Z(\tau)}K_3(t, u_{a,n-1}) + \frac{\tau}{Z(\tau)\Gamma(\tau)} \int_0^t (t-\zeta)^{\tau-1}K_3(\zeta, u_{a,n-1}) d\zeta, \end{cases} \quad (65)$$

where  $u_d(0), u_q(0),$  and  $u_a(0) \geq 0$ .

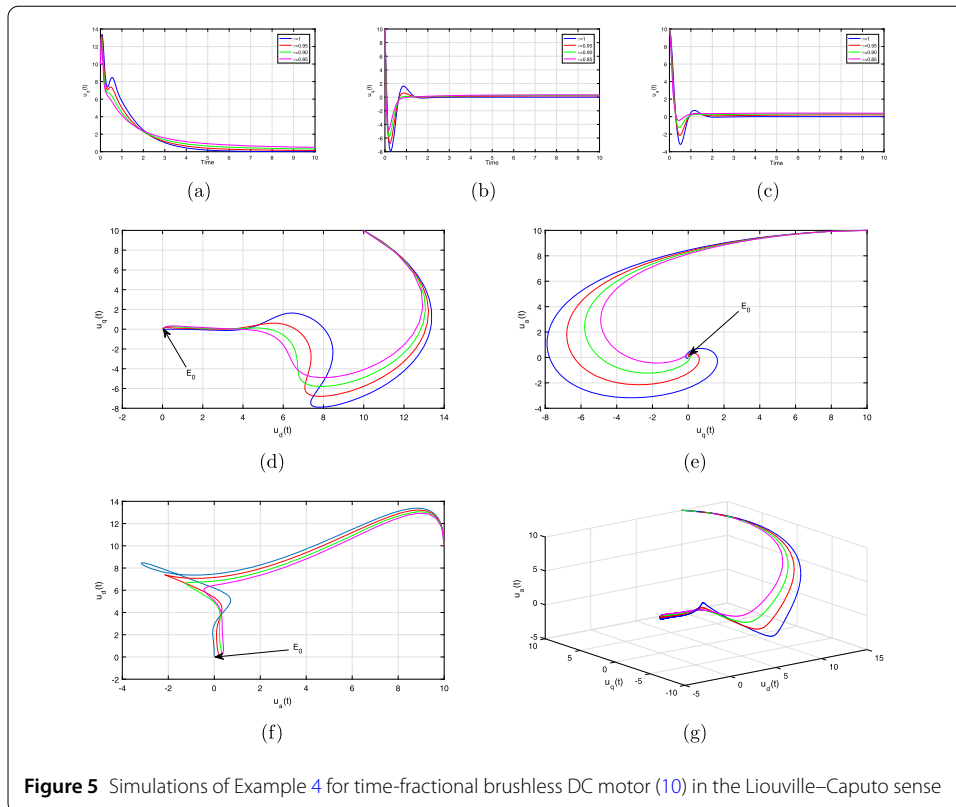


**Figure 5** Simulations of Example 4 for time-fractional brushless DC motor (10) in the Liouville–Caputo sense

Let the difference between successive components of system (65) be denoted by  $W(n, i)$ ,  $i = 1, 2, 3$ . Then from system (65) and the kernel equations satisfying the Lipschitz condition we have

$$\left\{ \begin{aligned} \|W_{n,1}\| &= \|u_{d,n}(t) - u_{d,n-1}(t)\| \\ &\leq \frac{(1-\tau)\eta_1}{Z(\tau)} \|u_{d,n-1}(t) - u_{d,n-2}(t)\| \\ &\quad + \frac{\tau\eta_1}{Z(\tau)\Gamma(\tau)} \int_0^t (t-\zeta)^{\tau-1} \|u_{d,n-1}(\zeta) - u_{d,n-2}(\zeta)\| d\zeta, \\ \|W_{n,2}\| &= \|u_{q,n}(t) - u_{q,n-1}(t)\| \\ &\leq \frac{(1-\tau)\eta_2}{Z(\tau)} \|u_{q,n-1}(t) - u_{q,n-2}(t)\| \\ &\quad + \frac{\tau\eta_2}{Z(\tau)\Gamma(\tau)} \int_0^t (t-\zeta)^{\tau-1} \|u_{q,n-1}(\zeta) - u_{q,n-2}(\zeta)\| d\zeta, \\ \|W_{n,3}\| &= \|u_{a,n}(t) - u_{a,n-1}(t)\| \\ &\leq \frac{(1-\tau)\eta_3}{Z(\tau)} \|u_{a,n-1}(t) - u_{a,n-2}(t)\| \\ &\quad + \frac{\tau\eta_3}{Z(\tau)\Gamma(\tau)} \int_0^t (t-\zeta)^{\tau-1} \|u_{a,n-1}(\zeta) - u_{a,n-2}(\zeta)\| d\zeta \end{aligned} \right. \tag{66}$$

or

$$\left\{ \begin{aligned} \|W_{n,1}\| &\leq \frac{(1-\tau)\eta_1}{Z(\tau)} \|W_{n-1,1}(t)\| + \frac{\tau\eta_1}{Z(\tau)\Gamma(\tau)} \int_0^t (t-\zeta)^{\tau-1} \|W_{n-1,1}(\zeta)\| d\zeta, \\ \|W_{n,2}\| &\leq \frac{(1-\tau)\eta_2}{Z(\tau)} \|W_{n-1,2}(t)\| + \frac{\tau\eta_2}{Z(\tau)\Gamma(\tau)} \int_0^t (t-\zeta)^{\tau-1} \|W_{n-1,2}(\zeta)\| d\zeta, \\ \|W_{n,3}\| &\leq \frac{(1-\tau)\eta_3}{Z(\tau)} \|W_{n-1,3}(t)\| + \frac{\tau\eta_3}{Z(\tau)\Gamma(\tau)} \int_0^t (t-\zeta)^{\tau-1} \|W_{n-1,3}(\zeta)\| d\zeta. \end{aligned} \right. \tag{67}$$

Using consequences (67), we can confirm the existence of the solution. □

**Theorem 4** Model (11) has a unique solution if

$$\frac{1 - \tau}{Z(\tau)} \eta_i + \frac{t_{max}^{\tau+1}}{\Gamma(\tau)Z(\tau)} \eta_i < 1 \quad \text{or} \quad 0 < 1 - \frac{t_{max}^{\tau+1}}{\Gamma(\tau)Z(\tau)} \eta_i - \frac{1 - \tau}{Z(\tau)} \eta_i, \quad i = 1, 2, 3.$$

*Proof* For the first equation in (11), let  $u_d(t)$  and  $u_{d,1}(t)$  be two solutions. Then

$$\begin{aligned} u_d(t) - u_{d,1}(t) &= \frac{1 - \tau}{Z(\tau)} (K_1(t, u_d) - K_1(t, u_{d,1})) \\ &\quad + \frac{\tau}{\Gamma(\tau)Z(\tau)} \int_0^t (t - \zeta)^{\tau-1} (K_1(\zeta, u_d) - K_1(\zeta, u_{d,1})) d\zeta, \\ \|u_d(t) - u_{d,1}(t)\| &\leq \frac{1 - \tau}{Z(\tau)} \|K_1(t, u_d) - K_1(t, u_{d,1})\| \\ &\quad + \frac{\tau}{\Gamma(\tau)Z(\tau)} \int_0^t (t - \zeta)^{\tau-1} \|K_1(\zeta, u_d) - K_1(\zeta, u_{d,1})\| d\zeta, \\ \|u_d(t) - u_{d,1}(t)\| &\leq \frac{(1 - \tau)\eta_1}{Z(\tau)} \|u_d - u_{d,1}\| + \frac{t^\tau \eta_1}{\Gamma(\tau)Z(\tau)} \|u_d(\zeta) - u_{d,1}(\zeta)\|. \end{aligned}$$

This implies

$$\left( 1 - \frac{(1 - \tau)\eta_1}{Z(\tau)} \eta_1 - \frac{(t^\tau)\eta_1}{Z(\tau)\Gamma(\tau)} \right) \|u_d(\zeta) - u_{d,1}(\zeta)\| \leq 0,$$

which implies that

$$\|u_d(\zeta) - u_{d,1}(\zeta)\| = 0, \quad \Rightarrow \quad u_d(\zeta) = u_{d,1}(\zeta).$$

Applying the same procedure to the remaining equations of (11), we obtain

$$\begin{aligned} \|u_q(\zeta) - u_{q,1}(\zeta)\| &= 0, \quad \Rightarrow \quad u_q(\zeta) = u_{q,1}(\zeta), \\ \|u_a(\zeta) - u_{a,1}(\zeta)\| &= 0, \quad \Rightarrow \quad u_a(\zeta) = u_{a,1}(\zeta). \end{aligned}$$

Thus the uniqueness of the fractional-order model is verified. □

### 13 The proposed numerical technique for Eq. (11)

This section is devoted to the numerical scheme, which is based on the rule [61], to solve the noninteger model (11). Let us consider ABC initial value problem of fractional (non-integer) order.

Let us consider the Liouville–Caputo noninteger initial value problem

$${}^{\text{ABC}}D_t^\tau U(t) = H(t, U(t)) \tag{68}$$

with initial condition  $U(t_0) = U_0$ , where  $H(t, U(t))$  is a continuous function. Applying the integral operator to all sides of equation (68) and the concept of ABC noninteger integral, we get the following Volterra integral equation:

$$U(t) - U(0) = \frac{1 - \tau}{Z(\tau)} H(t, U(t)) + \frac{\tau}{\Gamma(\tau)Z(\tau)} \int_0^t (t - \zeta)^{\tau-1} H(\zeta, U(\zeta)) d\zeta. \tag{69}$$

Taking  $t = t_n = nh$  in (69), where  $h$  is the step size, we get

$$U(t_n) - U(t_0) = \frac{1 - \tau}{Z(\tau)} H(t_n, U(t_n)) + \frac{\tau}{\Gamma(\tau)Z(\tau)} \sum_0^{n-1} \int_{t_0}^{t_n} t(t_n - \zeta)^{\tau-1} H(\zeta, U(\zeta)) d\zeta. \tag{70}$$

Now we can approximate the function  $H(\zeta, U(\zeta))$  with the help of the first-order Lagrange interpolation:

$$H(\zeta, U(\zeta)) \approx H(t_{i+1}, U_{i+1}) + \frac{\zeta - t_{i+1}}{h} (H(t_{i+1}, U_{i+1}) - H(t_i, U_i)), \quad \zeta \in [t_i, t_{i+1}], \tag{71}$$

where  $U_i = U(t_i)$ . Replacing (71) in (70) with some algebraic manipulations, we get the following ABC product-integration (ABCPI) formula [67]:

$$U_n = U_0 + \frac{\tau h^\tau}{Z(\tau)} \left( A_n H(t_0, U_0) + \sum_{i=1}^n B_{n-i} H(t_i, U_i) \right), \quad n \geq 1, \tag{72}$$

where

$$\begin{cases} A_n = \frac{(n-1)^\tau - n^\tau (n-\tau-1)}{\Gamma(\tau+2)}, \\ B_j = \begin{cases} \frac{1}{\Gamma(\tau+2)} + \frac{1-\tau}{\tau h^\tau}, & j = 0, \\ \frac{(j-1)^{\tau+1} - 2j^{\tau+1} + (j+1)^{\tau+1}}{\Gamma(\tau+2)}, & j = 1, 2, \dots, n-1. \end{cases} \end{cases} \tag{73}$$

The convergence order for the ABCPI rule is  $\tau + 1$ , that is, the inaccuracy satisfies  $|U(t_n) - U_n| = O(h^{1+\tau})$  [40, 67–70]. Note that we use discrete convolutions during the run of this process, which are assessed by considering the algorithm of FFT. It has the benefit that the computational cost is proportional to  $O(N \log^2 N)$  subject to  $O(N^2)$  as in any other prevalent discretization algorithm (see [26] and references therein).

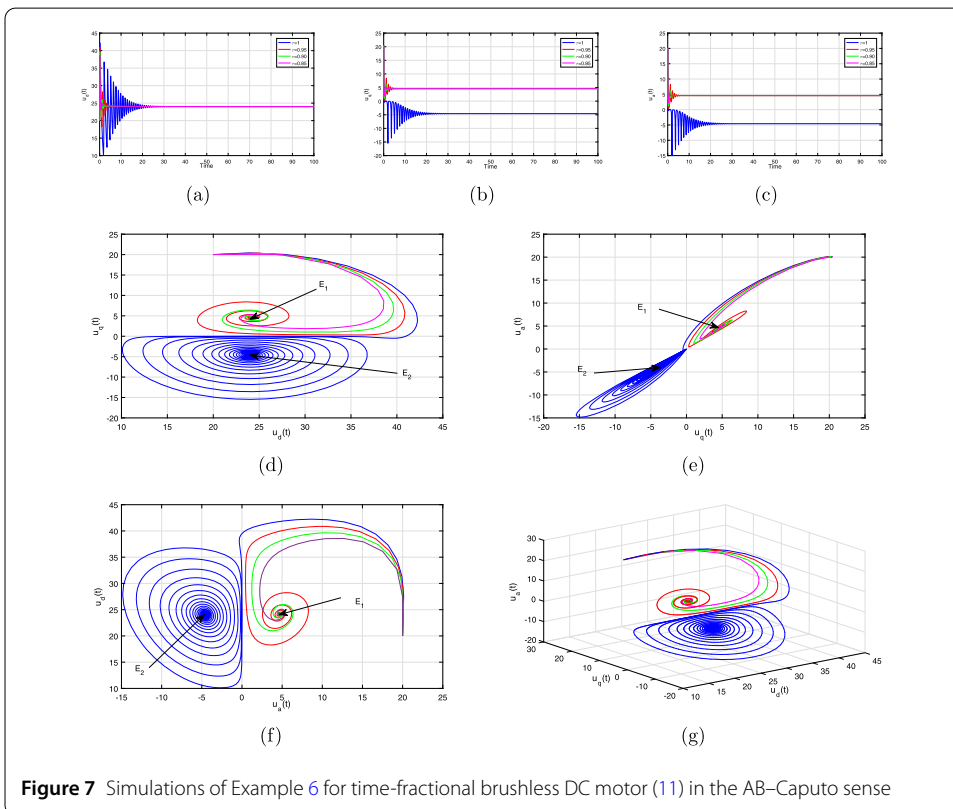
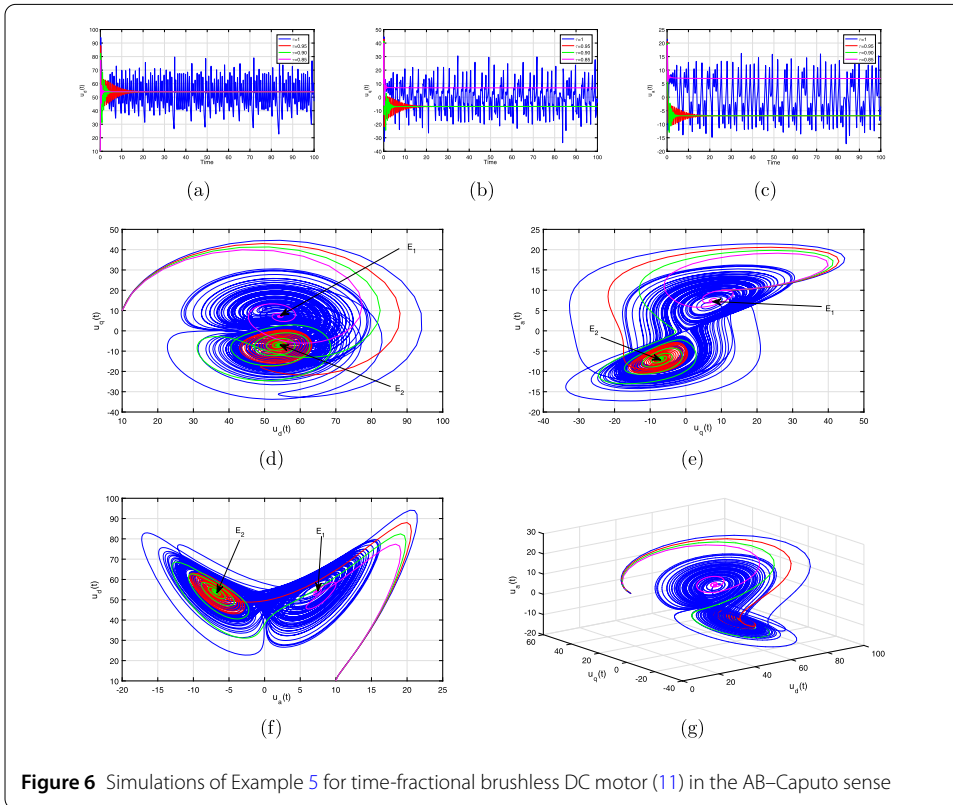
### 14 Numerical implementation for ABC-PI method on equation (11)

The following recursive formulas are obtained by applying the computational algorithm (72)–(73) to system (11):

$$\begin{cases} u_{d,n} = u_{d,0} + \frac{h^\tau \tau}{Z(\tau)} (A_n (-\sigma u_{d,0} + u_{q,0} u_{a,0}) + \sum_{i=1}^n B_{n-i} (-\sigma u_{d,i} + u_{q,i} u_{a,i})), \\ u_{q,n} = u_{q,0} + \frac{h^\tau \tau}{Z(\tau)} (A_n (-u_{q,0} + \beta u_{a,0} - u_{d,0} u_{a,0}) \\ \quad + \sum_{i=1}^n B_{n-i} (-u_{q,i} + \beta u_{a,i} - u_{d,i} u_{a,i})), \\ u_{a,n} = u_{a,0} + \frac{h^\tau \tau}{Z(\tau)} (A_n (\gamma u_{q,0} - \gamma u_{a,0}) + \sum_{i=1}^n B_{n-i} (\gamma u_{q,i} - \gamma u_{a,i})). \end{cases} \tag{74}$$

*Example 5* Taking the iterative arrangement (74), we consider the following values of the parameters [13, 18]:  $\sigma = 0.875$ ,  $\beta = 55$ , and  $\gamma = 4$  with initial conditions  $u_d(0) = 10$ ,  $u_q(0) = 10$ , and  $u_a(0) = 10$ . See Fig. 6.

*Example 6* Taking the iterative arrangement (74), we consider the following values of the parameters:  $\sigma = 0.875$ ,  $\beta = 25$ , and  $\gamma = 42$  with initial conditions  $u_d(0) = 20$ ,  $u_q(0) = 20$ , and  $u_a(0) = 20$ . See Fig. 7.



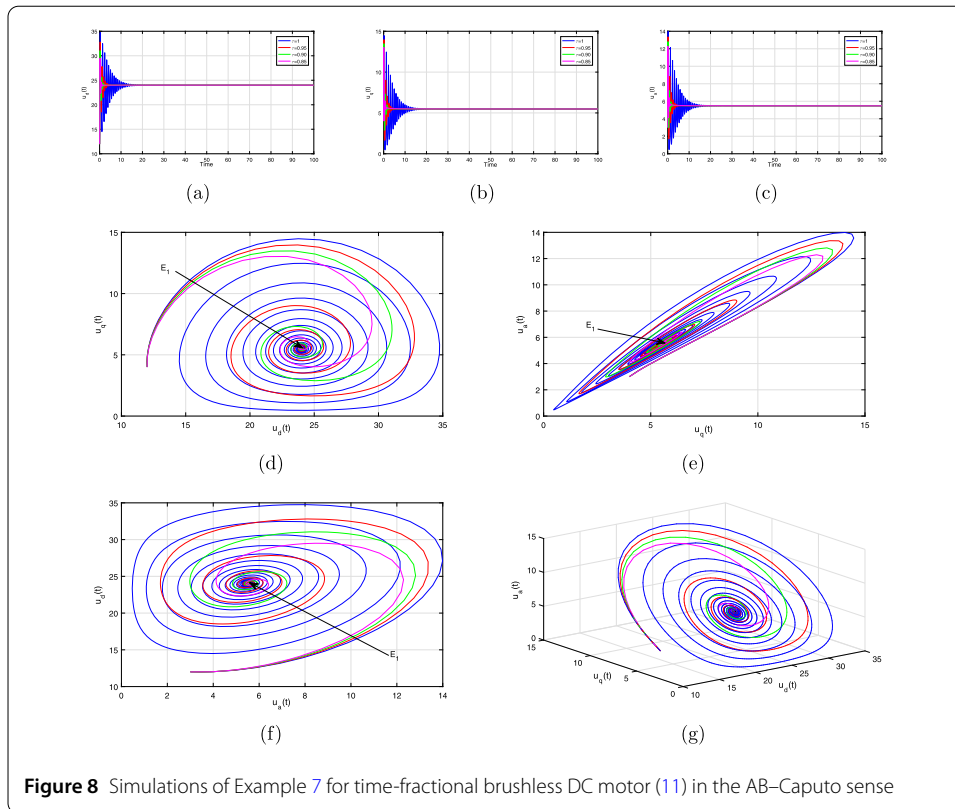


**Figure 8** Simulations of Example 7 for time-fractional brushless DC motor (11) in the AB–Caputo sense

*Example 7* Taking the iterative arrangement (74), we consider the following values of the parameters:  $\sigma = 1.25$ ,  $\beta = 25$ , and  $\gamma = 42$  with initial conditions  $u_d(0) = 12$ ,  $u_q(0) = 4$ , and  $u_a(0) = 3$ . See Fig. 8.

*Example 8* Taking the iterative arrangement (74), we consider the following values of the parameters:  $\sigma = 0.875$ ,  $\beta = 0.786$ , and  $\gamma = 4$  with initial conditions  $u_d(0) = 10$ ,  $u_q(0) = 10$ , and  $u_a(0) = 10$ . See Fig. 9.

### 15 Discussion and outcomes

In Example 1 or 5 of LC-PI and ABCPI, the parameters used are  $\sigma = 0.875$ ,  $\beta = 55$ , and  $\gamma = 4$ . The simulations of both numerical techniques are shown in Figs. 2(a–g) and 6(a–g). The system under observation converges to two equilibrium points  $E_1$  and  $E_2$  for different values of fractional order  $\tau$ . The simulations 2(a) and 6(a) for  $u_d$  reveal that the system is chaotic for  $\tau = 1$ , and it is not an attractor, but when the fractional order lowers down by 5%, the simulations indicate that the system becomes an attractor and converges to the equilibrium point  $E_1$ . The simulations 2(b), 2(c), 6(b), and 6(c) for  $u_q$  and  $u_a$  reveal that the system is chaotic for  $\tau = 1$ , for the fractional orders  $\tau = 0.95$  and  $\tau = 0.90$ , the system converges to  $E_2$  but for  $\tau = 0.85$ , the system converges to the other equilibrium point  $E_1$ . Also, these equilibrium points can easily be identified from 3D plots and 2D phase plots. These plots show that the DC motor system exhibits the butterfly effect.

In Example 2 or 6 of LC-PI and ABCPI, the parameters used are  $\sigma = 0.875$ ,  $\beta = 25$ , and  $\gamma = 42$ . The simulations of both numerical techniques are shown in Figs. 3(a–g) and 7(a–g). The simulations 3(a) and 7(a) for  $u_d$  reveal that the system is not chaotic for  $\tau =$

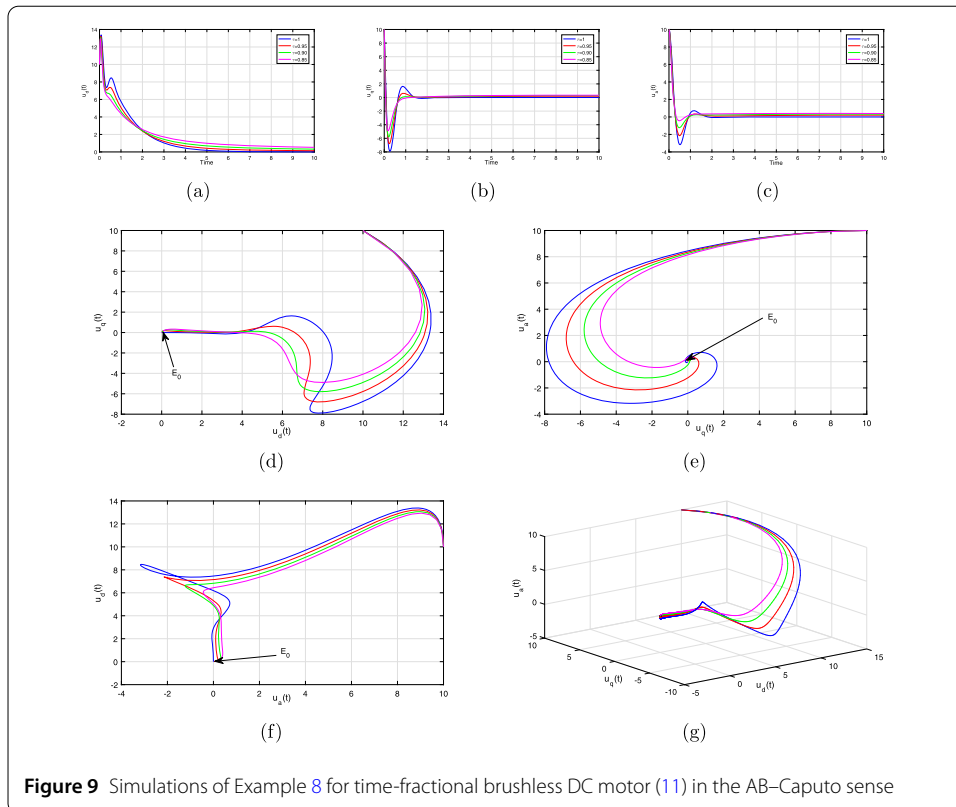


**Figure 9** Simulations of Example 8 for time-fractional brushless DC motor (11) in the AB–Caputo sense

1, 0.95, 0.90, and 0.85, and the system is an attractor and converges to the equilibrium point  $E_1$ . The simulations 3(b), 3(c), 7(b), and 7(c) for  $u_q$  and  $u_a$  reveal that the system converges to two equilibrium points  $E_1$  and  $E_2$ . These equilibrium points can easily be seen in 3D and 2D phase plots. These plots show that the DC motor system exhibits two wing simulations.

In Example 3 or 7 of LC-PI and ABCPI, the parameters used are  $\sigma = 1.25$ ,  $\beta = 25$ , and  $\gamma = 42$ . The simulations of both numerical methods are shown in Figs. 4(a–g) and 8(a–g). The fractional system (10)–(11) converges to one equilibrium point, that is,  $E_1 = (\beta - 1, \sqrt{\sigma(\beta - 1)}, \sqrt{\sigma(\beta - 1)})$  for different values of noninteger order  $\tau$ . Figure 4(d–g) and 8(d–g) show the 2D and 3D effects, which are in spiral shape and converge to  $E_1$ .

In Example 4 or 8 of LC-PI and ABCPI, the parameters used are  $\sigma = 0.875$ ,  $\beta = 0.786$ , and  $\gamma = 4$ . The simulations of both numerical methods are given in Figs. 5(a–g) and 9(a–g). The fractional system (10)–(11) converges to one equilibrium point  $E_0$  for all values of noninteger order  $\tau$ . Here  $E_0$  is the trivial equilibrium point.

### 16 Conclusion

In this paper, we considered two iterative techniques, the Caputo–Liouville product integration (CL-PI) and Atangana–Baleanu–Caputo product integration (ABCPI) rules for solving brushless DC motor model. The noninteger definitions of Liouville–Caputo and Atangana–Baleanu types are taken into account to model the proposed system. Moreover, kernels considered in such classes of operators are the Mittag-Leffler and power-law functions, respectively. Next, the order of the noninteger derivative discussed in both operators has a very important part in the outcomes attained from the corresponding meth-

ods. The numerical consequences and theoretical considerations are compared to infer that both derivatives are very favorable tools to analyze the exemplary. The equilibrium analysis of the system is discussed, which is useful to confirm the numerical imitations. The operators used and the techniques offered in this paper can be used to solve many other problems. The future research direction is to use the ABCPI technique in image processing and stochastic differential equations.

#### Acknowledgements

The authors are thankful to the editorial board and the anonymous reviewers whose comments improved the quality of the paper.

#### Funding

This research was not supported by any project.

#### Availability of data and materials

All of the authors declare that there is no data for the numerical simulation section.

#### Competing interests

The authors declare that they have no competing interests.

#### Authors' contributions

All authors read and approved the final manuscript.

#### Author details

<sup>1</sup>Department of Mathematics, Faculty of Sciences, University of Central Punjab, Lahore, Pakistan. <sup>2</sup>Department of Mathematics, University of Malakand, Chakdara, Dir (lower), KPK, Pakistan. <sup>3</sup>Department of Mathematics, Faculty of Science, Van Yuzuncu Yil University, 65080, Van, Turkey.

#### Publisher's Note

Springer Nature remains neutral with regard to jurisdictional claims in published maps and institutional affiliations.

Received: 6 April 2021 Accepted: 14 July 2021 Published online: 30 September 2021

#### References

1. Podlubny, I.: *Fractional Differential Equations*. Academic Press, San Diego (1999)
2. Hilfer, R.: *Applications of Fractional Calculus in Physics*. World Scientific, Singapore (2000)
3. Chen, L.P., He, Y.G., Chai, Y., Wu, R.C.: New results on stability and stabilization of a class of nonlinear fractional-order systems. *Nonlinear Dyn.* **75**, 633 (2014)
4. Aghababa, M.P., Aghababa, H.P.: The rich dynamics of fractional-order gyros applying a fractional controller. *Proc. Inst. Mech. Eng., Part I, J. Syst. Control Eng.* **227**, 588 (2013)
5. Aghababa, M.P.: Chaos in a fractional-order micro-electro-mechanical resonator and its suppression. *Chin. Phys. B* **21**, 100505 (2012)
6. Hartley, T.T., Lorenzo, C.F., Qammer, H.K.: Chaos in a fractional order Chua's system. *IEEE Trans. Circuits Syst. I, Regul. Pap.* **42**, 485 (1995)
7. Jia, H.Y., Chen, Z.Q., Qi, G.Y.: Chaotic characteristics analysis and circuit implementation for a fractional-order system. *IEEE Trans. Circuits Syst. I, Regul. Pap.* **61**, 845 (2014)
8. Kiani, B.A., Fallahi, K., Pariz, N., Leung, H.: A chaotic secure communication scheme using fractional chaotic systems based on an extended fractional Kalman filter. *Commun. Nonlinear Sci. Numer. Simul.* **14**, 863 (2009)
9. Muthukumar, P., Balasubramaniam, P., Ratnavelu, K.: Synchronization of a novel fractional order stretch-twist-fold (STF) flow chaotic system and its application to a new authenticated encryption scheme (AES). *Nonlinear Dyn.* **77**, 1547 (2014)
10. Hemati, N., Leu, M.C.: A complete model characterization of brushless DC motors. *IEEE Trans. Ind. Appl.* **28**, 172 (1992)
11. Hemati, N.: Strange attractors in brushless DC motors. *IEEE Trans. Circuits Syst. I, Regul. Pap.* **41**, 40 (1994)
12. Ge, Z.M., Chang, C.M., Chen, Y.S.: Anti-control of chaos single time scale brushless DC motors and chaos synchronization of different order system. *Chaos Solitons Fractals* **27**, 1298–1315 (2006)
13. Wei, D.Q., Wan, L., Luo, X.S., Zeng, S.Y., Zhang, B.: Global exponential stabilization for chaotic brushless DC motors with a single input. *Nonlinear Dyn.* **77**, 209 (2014)
14. Abdel Aty, A.M., Azar, A.T., Vaidyanathan, S., Ouannas, A., Radwan, A.G.: Application of continuous-time fractional order chaotic systems In: *Mathematical techniques of fractional order system*. Chap. 14 (2018). <https://doi.org/10.1016/B978-0-12-813592-1.00014-3>
15. Narmada, R., Arounassalame, M.: Design and performance evaluation of fractional order controller for brushless DC motor. *Int. J. Electr. Eng. Inform.* **6**(3), 606–617 (2014)
16. Shen, S., Zhou, P.: Synchronization of the fractional order brushless DC motors chaotic system. *J. Control Sci. Eng.* **2016**, 1236210 (2016)
17. Atangana, A., Qureshi, S.: Modeling attractors of chaotic dynamical systems with fractal-fractional operators. *Chaos Solitons Fractals* **123**, 320–337 (2019)

18. Zhou, P, Bai, R., Zheng, J.: Stabilization of a fractional-order chaotic brushless DC motor via a single output. *Nonlinear Dyn.* **82**, 519–525 (2015). <https://doi.org/10.1007/s11071-015-2172-4>
19. El-Ajou, A., Oqielat, M.N., Al-Zhour, Z., Kumar, S., Momani, S.: Solitary solutions for time-fractional nonlinear dispersive PDEs in the sense of conformable fractional derivative. *Chaos* **29**, 093102 (2019)
20. Odibat, Z., Kumar, S.: A robust computational algorithm of homotopy asymptotic method for solving systems of fractional differential equations. *J. Comput. Nonlinear Dyn.* **14**(8), 081004 (2019)
21. Kumar, R., Kumar, S.: A new fractional modelling on susceptible-infected recovered equations with constant vaccination rate. *Nonlinear Eng.* **3**(1), 11–19 (2014)
22. Kumar, S.: A new efficient algorithm to solve non-linear fractional Itô coupled system and its approximate solution. *Walailak J. Sci. Technol.* **11**(12), 1057–1067 (2014)
23. Gao, W., Ghanbari, B., Baskonus, H.M.: New numerical simulations for some real world problems with Atangana–Baleanu fractional derivative. *Chaos Solitons Fractals* **128**, 34–43 (2019)
24. Ghanbari, B., Gomez-Aguilar, J.F.: Modeling the dynamics of nutrient phytoplankton-zooplankton system with variable-order fractional derivatives. *Chaos Solitons Fractals* **116**, 114–120 (2018)
25. Allahviranloo, T., Ghanbari, B.: On the fuzzy fractional differential equation with interval Atangana–Baleanu fractional derivative approach. *Chaos Solitons Fractals* **130**, 109397 (2020)
26. Baba, I.A., Ghanbari, B.: Existence and uniqueness of solution of a fractional order tuberculosis model. *Eur. Phys. J. Plus* **134**(10), 489 (2019)
27. Jajarmi, A., Ghanbari, B., Baleanu, D.: A new and efficient numerical method for the fractional modelling and optimal control of diabetes and tuberculosis coexistence. *Chaos* **29**, 093111 (2019)
28. Bonyah, E., Atangana, A., Chand, M.: Analysis of 3D IS-LM macroeconomic system model within the scope of fractional calculus. *Chaos Solitons Fractals X* **2**, 100007 (2019)
29. Bonyah, E., Khan, M.A., Okosun, K.O., Gomez-Aguilar, J.F.: Modelling the effects of heavy alcohol consumption on the transmission dynamics of gonorrhoea with optimal control. *Math. Biosci.* **309**, 1–11 (2019)
30. Salari, A., Ghanbari, B.: Existence and multiplicity for some boundary value problems involving Caputo and Atangana–Baleanu fractional derivatives: a variational approach. *Chaos Solitons Fractals* **127**, 312–317 (2019)
31. Atangana, A., Bonyah, E.: Fractional stochastic modeling: new approach to capture more heterogeneity. *Chaos* **29**(1), 013118 (2019)
32. Qureshi, S., Bonyah, E., Shaikh, A.A.: Classical and contemporary fractional operators for modeling diarrhea transmission dynamics under real statistical data. *Physica A* **535**, 122496 (2019)
33. Zafar, Z.U.A., Younas, S., Hussain, M.T., Tunç, C.: Fractional aspects of coupled mass-spring system. *Chaos Solitons Fractals* **144**, 110677 (2021)
34. Zafar, Z.U.A., Ali, N., Zaman, G., Thounthong, P., Tunç, C.: Analysis and numerical simulations of fractional order Vallis system. *Alex. Eng. J.* **59**, 2591–2605 (2021)
35. Caputo, M., Mainardi, F.: A new dissipation model based on memory mechanism. *Pure Appl. Geophys.* **91**, 134–147 (1971)
36. Hadamard, J.: Essai sur l'étude des fonctions données par leur développement de Taylor. *J. Math. Pures Appl.* **8**, 101–186 (1892)
37. Gerolymatou, E., Vardoulakis, I., Hilfer, R.: Modelling infiltration by means of a nonlinear fractional diffusion model. *J. Phys. D, Appl. Phys.* **39**(8), 4104–4110 (2006)
38. Atangana, A., Baleanu, D.: New fractional derivatives with nonlocal and nonsingular kernel: theory and application to heat transfer model. *Therm. Sci.* **20**(2), 763–769 (2016)
39. Atangana, A.: Non validity of index law in fractional calculus: a fractional differential operator with Markovian and non-Markovian properties. *Physica A* **505**, 688–706 (2018)
40. Ghanbari, B., Atangana, A.: A new application of fractional Atangana–Baleanu derivatives: designing ABC-fractional masks in image processing. *Physica A* **542**, 123516 (2020)
41. Baleanu, D., Jajarmi, A., Bonyah, E., Hajjipour, M.: New aspects of the poor nutrition in the life cycle within the fractional calculus. *Adv. Differ. Equ.* **2018**, 230 (2018)
42. Baleanu, D., Jajarmi, A., Hajjipour, M.: On the nonlinear dynamical systems within the generalized fractional derivatives with Mittag-Leffler kernel. *Nonlinear Dyn.* **94**(1), 397–414 (2018)
43. Yusuf, A., Qureshi, S., Inc, M., Aliyu, A.I., Baleanu, D., Shaikh, A.A.: Two strain epidemic model involving fractional derivative with Mittag-Leffler kernel. *Chaos* **28**(12), 123121 (2018)
44. Bonyah, E., Atangana, A., Elsadany, A.A.: A fractional model for predator–prey with omnivore. *Chaos* **29**(1), 013136 (2019)
45. Slynko, V., Tunç, C.: Stability of abstract linear switched impulsive differential equations. *Automatica* **107**, 433–441 (2019)
46. Tunç, C., Tunç, O.: A note on certain qualitative properties of a second order linear differential system. *Appl. Math. Inf. Sci.* **9**(2), 953–956 (2015)
47. Tunç, C.: Stability and boundedness of solutions to non-autonomous delay differential equations of third order. *Nonlinear Dyn.* **62**(4), 945–953 (2010)
48. Tunç, C., Tunç, O., Wang, Y., Yao, J.C.: Qualitative analyses of differential systems with time-varying delays via Lyapunov–Krasovskii approach. *Mathematics* **9**(11), 1196 (2021)
49. Tunç, C., Tunç, O.: On the stability, integrability and boundedness analyses of systems of integro-differential equations with time-delay retardation. *Rev. R. Acad. Cienc. Exactas Fis. Nat., Ser. A Mat.* **15**(3), 115 (2021)
50. Tunç, O., Atan, O., Tunç, C., Yao, J.C.: Qualitative analyses of integro-fractional differential equations with Caputo derivatives and retardations via the Lyapunov–Razumikhin method. *Axioms* **10**(2), 58 (2021). <https://doi.org/10.3390/axioms10020058>
51. Tunç, C., Tunç, O., Wang, Y.: Delay-dependent stability, integrability and boundedness criteria for delay differential systems. *Axioms* **10**(3), 138 (2021). <https://doi.org/10.3390/axioms10030138>
52. Khan, H., Tunç, C., Khan, A.: Stability results and existence theorems for nonlinear delay-fractional differential equations with  $\phi * p$ -operator. *J. Appl. Anal. Comput.* **10**(2), 584–597 (2020)
53. Bohner, M., Tunç, O., Tunç, C.: Qualitative analysis of Caputo fractional integro-differential equations with constant delays. *Comput. Appl. Math.* **40**, 214 (2021). <https://doi.org/10.1007/s40314-021-01595-3>

54. Graef, J.R., Tunç, C., Şevli, H.: Razumikhin qualitative analyses of Volterra integro-fractional delay differential equation with Caputo derivatives. *Commun. Nonlinear Sci. Numer. Simul.* (2021). <https://doi.org/10.1016/j.cnsns.2021.106037>
55. Tunç, O.: On the behaviors of solutions of systems of non-linear differential equations with multiple constant delays. *Rev. R. Acad. Cienc. Exactas Fis. Nat., Ser. A Mat.* **115**, 164 (2021). <https://doi.org/10.1007/s13398-021-01104-5>
56. Li, H.L., Zhang, L., Hu, C., Jiang, Y.L., Teng, Z.: Dynamical analysis of a fractional order predator–prey model incorporating a prey refuge. *J. Appl. Math. Comput.* **54**, 435–449 (2017)
57. Ahmed, E., El-Sayed, A.M.A., El-Saka, H.A.A.: On some Routh–Hurwitz conditions for fractional order differential equations and their applications in Lorenz, Rossler, Chua Chen systems. *Phys. Lett. A* **358**, 1–4 (2006)
58. Podlubny, I.: *Fractional Differential Equations: An Introduction to Fractional Derivatives, Fractional Differential Equations, to Methods of Their Solution and Some of Their Applications*, vol. 198. Academic Press, New York (1998)
59. Diethelm, K.: *The Analysis of Fractional Differential Equations: An Application-Oriented Exposition Using Differential Operators of Caputo Type*. Springer, Berlin (2010)
60. Zeidler, E.: *Non-linear Functional Analysis and Its Application*. Springer, New York (1986)
61. Young, A.: Approximate product-integration. *Proc. R. Soc. Lond. Ser. A* **224**, 552–561 (1954)
62. Garrappa, R.: On linear stability of predictor–corrector algorithms for fractional differential equations. *Int. J. Comput. Math.* **87**(10), 2281–2290 (2010)
63. Hairer, E., Lubich, C., Schlichte, M.: Fast numerical solution of nonlinear Volterra convolution equations. *SIAM J. Sci. Stat. Comput.* **6**(3), 532–541 (1985)
64. Diethelm, K., Ford, N.J., Freed, A.D.: Detailed error analysis for a fractional Adams method. *Numer. Algorithms* **36**(1), 31–52 (2004)
65. Popolizio, M.: Numerical solution of multiterm fractional differential equations using the matrix Mittag-Leffler functions. *Mathematics* **6**(1), 7 (2018)
66. Garrappa, R.: Numerical solution of fractional differential equations: a survey and a software tutorial. *Mathematics* **6**(2), 16 (2018)
67. Ghanbari, B., Kumar, D.: Numerical solution of predator-prey model with Beddington–DeAngelis functional response and fractional derivatives with Mittag-Leffler kernel. *Chaos, Interdiscip. J. Nonlinear Sci.* **29**, 063103 (2019)
68. Ghanbari, B., Gomez-Aguilar, J.F.: Analysis of two avian influenza epidemic models involving fractal-fractional derivatives with power and Mittag-Leffler memories. *Chaos, Interdiscip. J. Nonlinear Sci.* **29**, 123113 (2019)
69. Ghanbari, B., Djilali, S.: Mathematical and numerical analysis of a three-species predator–prey model with herd behavior and time fractional-order derivative. *Math. Methods Appl. Sci.* **43**(4), 1736–1752 (2019)
70. Ghanbari, B., Atangana, A.: Some new edge detecting techniques based on fractional derivatives with non-local and non-singular kernels. *Adv. Differ. Equ.* **2020**, 435 (2020)

Submit your manuscript to a SpringerOpen<sup>®</sup> journal and benefit from:

- Convenient online submission
- Rigorous peer review
- Open access: articles freely available online
- High visibility within the field
- Retaining the copyright to your article

---

Submit your next manuscript at ► [springeropen.com](https://www.springeropen.com)

---